Macromolecular multi-chromophoric scaffolding

Erik Schwartz, Stéphane Le Gac,† Jeroen J. L. M. Cornelissen,‡ Roeland J. M. Nolte* and Alan E. Rowan*

Received 22nd October 2009
First published as an Advance Article on the web 2nd March 2010
DOI: 10.1039/b922160c

This *critical review* describes recent efforts in the field of chromophoric scaffolding. The advances in this research area, with an emphasis on rigid scaffolds, for example, synthetic polymers, carbon nanotubes (CNTs), nucleic acids, and viruses, are presented (166 references).

1. Introduction

Chromophores are of pivotal importance in nature and play a fundamental role in many aspects of life, such as photosynthesis and the processes within the circulatory system. They also act as dyes and pigments in a wide variety of technological applications. In many of these applications, the organisation of chromophores is of crucial importance for the performance of the assembly or device. To arrange the chromophores into functional architectures scientists have developed numerous approaches for the precise positioning of chromophoric building blocks and these have been applied extensively in the last years, in particular, in the field of the material sciences.[1,2] The aim of this aforementioned research is to control the electronic interactions between adjacent chromophoric units and thereby obtain materials with unique properties and potentially new applications.[3,4] Often the very elegant and essential chromophoric arrays that can be found in nature are used as a source of inspiration and sometimes as a blueprint for synthetic systems. A particular example is the photosynthetic system in which chlorophyll and bacteriochlorophyll chromophores are organised in such a way that the transfer of excitation energy and electrons occurs with a very high efficiency over large distances. This architecture–function relationship is also beautifully illustrated by the circular antenna complex of the purple bacteria light-harvesting complex 2 (LH2),[5] which displays an incredible efficiency towards the harvesting of sunlight. The precise organisation of the two ring-shaped arrays of chlorophylls allows for an efficient energy transfer from the outer- to the inner-ring and finally to the photosynthetic reaction centre where energy separation occurs.[6] The combination of the perfectly tuned energy gradient,

Institute for Molecules and Materials, Radboud University Nijmegen, Heyendaalseweg 135, 6525 AJ, The Netherlands.
E-mail: r.nolte@science.ru.nl, a.rowan@science.ru.nl
† Present address: Sciences Chimiques de Rennes, UMR CNRS 6226, Université de Rennes 1, 35042 Rennes Cedex, France.
‡ Present address: Laboratory for Biomolecular Nanotechnology, MESA+ Institute, Faculty of Science & Technology, University of Twente, P.O. Box 217, 7500 AE Enschede, The Netherlands.

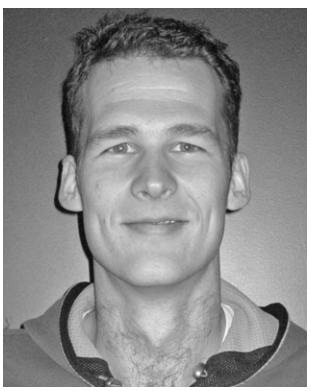

Erik Schwartz

Erik Schwartz was born on 14 August 1980, in The Netherlands. He studied chemistry at the Radboud University Nijmegen, where he obtained his master degree in 2005, graduating cum laude. Since 2005 he has been doing his PhD thesis at the same university working on the synthesis and characterisation of helical polyisocyanopeptides under the supervision of Prof. Roeland Nolte, Prof. Alan Rowan and Prof. Jeroen Cornelissen. As of February 2010 Erik will be affiliated with the Scripps Research Institute in La Jolla, California, where he will be working on the development of stable synthetic antibodies, for which he received both a RUBICON fellowship and a post-doctoral fellowship from Schering-Plough. Erik Schwartz is the first recipient of this Schering-Plough award, recently established to support a PhD student from The Netherlands as post-doctoral researcher at a university within the United States.

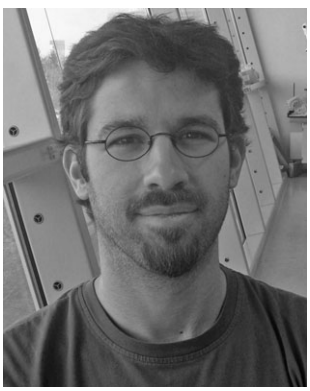

Stéphane Le Gac

Stéphane Le Gac completed his PhD in organic chemistry in 2006 under the supervision of Prof. I. Jabin, at Le Havre University (France). He started a first postdoctoral period at the Free University of Brussels (Belgium) under the supervision of Prof. A. Kirsch-De Mesmaeker, working with ruthenium-oligonucleotide photo-reagents. He then moved to Nijmegen (The Netherlands) as a postdoctoral fellow in the groups of Prof. R. Nolte and Prof. A. Rowan, aiming at the development of new strategies for the functionalisation of helical polymers (polyisocyanides). In 2009, he was appointed CNRS researcher at the University of Rennes (France). His current interest lies in the design of novel macromolecular scaffolds for therapeutic applications.

the precisely interacting chromophores, the ability to store excess energy temporarily within the light-harvesting complex 1 (LH1) ring and the absorption of the solar light over a wide wavelength range makes this system extremely efficient (>95%) for absorbing photons (Fig. 1).[7–11] The efficiency of this antenna is not only a result of the chromophores that are used but also relies on their precise orientation and positioning relative to one other. The positioning of the chromophores is controlled by the protein biomolecular scaffold; this has inspired many researchers over the last decades to create artificial systems in which chromophores are ordered and the unique properties of the structures are utilised. Several approaches to achieve high levels of chromophoric ordering within molecular systems, with the hope of creating efficient energetic interactions, have been attempted, based on for example, dendritic,[12,13] supramolecular,[14] or covalent systems.[15] Another approach, which combines the last two approaches, is to use rigid scaffolds that possess supramolecular features, which can be used to precisely organise the chromophores. The focus of this review is on the arrangement of extended π-conjugated chromophores, such as porphyrins, phthalocyanines, perylenes or pyrenes, by using rigid helical polymers, carbon nanotubes (CNTs), which for this review we consider to be a polycarbon species, nucleic acids and viruses. The advantages and limitations of such approaches will be discussed.

Jeroen J. L. M. Cornelissen

Jeroen J. L. M. Cornelissen is Professor of Biomolecular Nanotechnology at the University of Twente. He obtained his PhD in 2001 from the University of Nijmegen, the Netherlands under the supervision of Prof. Roeland Nolte and did post-doctoral work at the IBM Almaden Research Center in San Jose, CA. In 2002 he returned to Nijmegen as an Assistant Professor before he took up his present position in 2009. His research interests are in the fields of protein-polymer biohybrids and protein cages as functional materials and confined reaction spaces. Prof. Cornelissen is the recipient of Veni & Vidi Innovative Research Grants and a EURYI Award and is a member of the advisory board of the Journal of Materials Chemistry.

2. Rigid helical polymers

One approach towards the ordering of chromophores is to make use of a synthetic polymer scaffold. Although linear polymers can be readily functionalised with dyes,[16,17] their overall architectural definition is often limited because they are flexible and can suffer from defects that may result in the formation of energy sinks. More attractive candidates for the arrangement of chromophores in well-defined arrays are rigid polymers, which are often helical.[18,19] The helix is one of the most important and basic structural motifs found in nature. The biological activities of biomacromolecules, such as proteins and nucleic acids, often depend on the presence of helical conformations. Also the function and physical properties of synthetic helical polymers are strongly correlated with the conformation of their macromolecular chains. Over the last 60 years, after the first discovery of a synthetic helical

Roeland J. M. Nolte

Roeland J. M. Nolte is Professor of Organic Chemistry at the Radboud University Nijmegen, The Netherlands, and Director of the Institute for Molecules and Materials. He is a member of the Royal Netherlands Academy of Science and holds a special Royal Academy of Science Chair in Chemistry. His research interests span a broad range of topics at the interfaces of Supramolecular Chemistry, Macromolecular Chemistry, and Biomimetic Chemistry, in which he focuses on the design of catalysts and (macro) molecular materials. His contributions to science have been recognized with numerous award lectureships and several national and international prizes including the Izatt-Christensen Award for Excellence in Macrocyclic Chemistry, the first Royal Netherlands Academy of Science Chair in Chemistry, and a knighthood in 2003. He has served on the editorial boards of many scientific journals, including the journal Science (Washington) and the RSC journal Chemical Communications (as Chairman).

Alan E. Rowan

Professor Dr Alan Rowan (seen in picture not eating melon) studied at the University of Liverpool, England, where he obtained a BSc 1st Honours in Chemistry and then a PhD in Physical Organic Chemistry. In 1992 he moved to New Zealand where he completed a Post doctoral study in the field of Supramolecular chemistry with Prof C. Hunter. In 1994 he moved to Nijmegen the Netherlands as a Marie Curie Fellow, and then as Assistant and Associate Professor with Prof R. J. Nolte. In 2005, he set up a new department of Molecular Materials in the Institute for Molecules and Materials, Nijmegen. His interests are in the relationship between molecular architecture and function, in self-assembling and macromolecular (bio)-organic and magnetic materials.

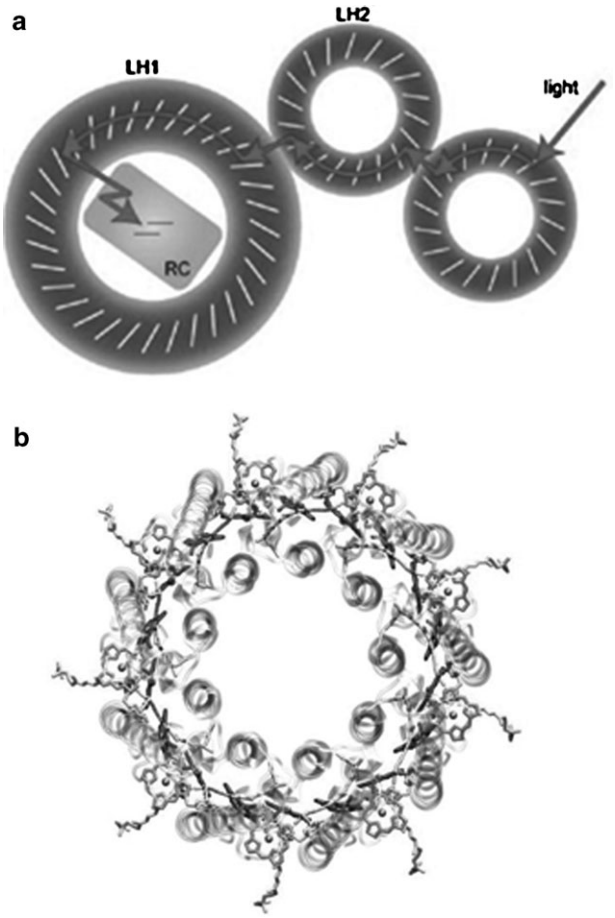

Fig. 1 (a) The transfer of a photon of light from the LH2 complexes through the LH1 complex and finally to the central photosynthetic reaction centre (RC). (b) The crystal structure of the LH2 of purple bacteria *Rhodopseudomonas acidophila*, which reveals a highly ordered array of chlorophyll molecules held in the required orientation by the peptidic alpha helices. Three bacteriochlorophyll molecules are associated with each pair of helices. (*Adapted with permission from ref. 51 Copyright 2006, Wiley-VCH.*)

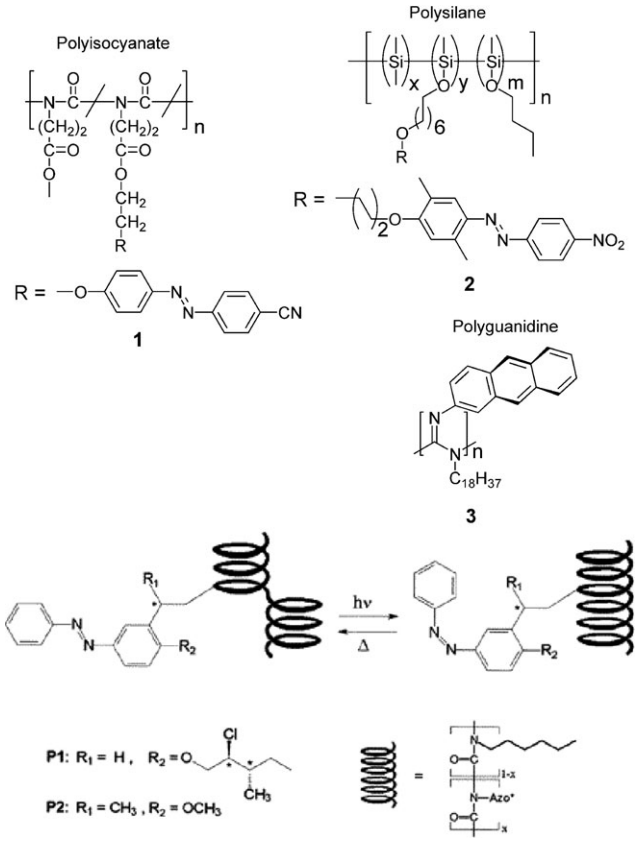

Chart 1 Chemical structures of the azo-benzene and anthracene based dynamic polymers **1–3** and the switching process in the chiral photochromic polyisocyanate copolymer. (*Adapted with permission from ref. 26 Copyright 1998, American Chemical Society.*)

polymer by Natta in 1955,[20] a variety of helical polymers have been developed. In this review the emphasis will be on helical polymers that have been used as scaffolds for the organisation of chromophores into well-defined architectures. Although a host of helical polyacetylenes have been prepared, this class of polymers will not be discussed since they are rather flexible in contrast to other classes of helical polymers, such as polyisocyanates, polyisocyanides, polysilanes or polyguanidines. For an excellent overview on work conducted with polyacetylenes see the reviews by Tang[21] and Yashima.[22,23] The basic characteristics of the polymers that are described in this section have been discussed in the literature,[18,22] therefore only a brief description of the polymers is given here.

One class of helical polymers are the polyisocyanates,[24] which are characterised by an *N*-substituted amide repeat unit and an 8_3 helical conformation (Chart 1). These polymers have a low helix inversion barrier and are therefore dynamic in nature. The majority of investigated polyisocyanates are not functionalised and consist mainly of alkyl or aryl derivatives. The lack of functionalised polyisocyanates is ascribed to the harsh conditions required for the preparation of the monomer and to the anionic nature of the polymerisation reactions, which are not compatible with many functional groups. To overcome these problems, an azo-chromophore dye was introduced in the polymer chain by a trans-esterification reaction involving the methyl ester of the polymer.[25] The resulting polymer **1** (Chart 1) had a functionalisation degree of 30% and displayed a tenfold increase in the optical rotation value. This indicates that the chromophores attached to the polyisocyanate are in a helical environment. Unfortunately, no further photophysical studies were undertaken to obtain a more detailed picture of the arrangement of the chromophores. In related work, chiral azo dyes were introduced into the polymeric system by the copolymerisation of an azo dye derivatised isocyanate with hexylisocyanate (Chart 1). The change in the helical conformation of the polyisocyanate backbone when triggered by the photoinduced isomerisation of the side chains was studied. For example, the chiroptical properties and the correlation between the helicity of the main chain and the photoisomerization of the side groups were studied by Circular Dichroism (CD) measurements.[26,27] It was apparent that at low concentrations of the chiral azo side groups, a linear relationship was present between the ratio of *cis* and *trans* isomers and the preference for one particular helical conformation. At higher concentrations of the chiral azo side groups, the stronger inducing species (*i.e.*, the *cis* isomer) dictated the helical conformation, in agreement with the

sergeant and soldier principle found by Green and co-workers in polyisocyanates.[24,28] Polysilanes possess a unique Si σ-conjugated backbone and like the polyisocyanates also belong to the class of dynamic helical polymers (Chart 1).[29] They are generally synthesised by simple Wurtz coupling reactions. The type of side chains in the polysilane has a dramatic influence on the rigidity, stability and optical properties of the polymer. A feature of polysilanes, shared with polyisocyanates, is the difficulty of synthesising derivatives with a wide variety of functionalities. The rigorous reaction conditions allow only alkyl or aryl substituents as side chains. To overcome this problem, Qin and co-workers partially replaced the Si–alkyl group of the polymer backbone by Si–Cl groups. Subsequent etherification with diphenyl azo dyes (Chart 1) resulted in the highly chromophore-loaded (>50%) polymer **2** (Chart 1), which showed a photoconductivity of 1.7 pS cm^{-1}, three orders of magnitude higher than the dark conductivity of simple polysilanes.[30]

Another class of helical polymers are the polyguanidines, which have been extensively explored by the group of Novak (Chart 1).[31–36] These polymers adopt a 6_1 helical conformation and are usually prepared by the (chiral) titanium catalysed polymerisation of carbodiimides. Stable helices with length up to 3 μm can be obtained by the incorporation of sterically demanding anthracene units, which can also act as UV-Vis chromophores allowing the close investigation of the polymer conformations.[36] Polymer **3** (Chart 1) exhibited a reversible, temperature and solvent-induced chiroptical switching behaviour due to a cooperative effect between the anthracene units (Fig. 2), as visualised by a blue/red shift in the UV-Vis absorption peaks (at 25 °C: λ_{max} = 384.4 nm and ε = 5400 M^{-1}; at 60 °C: λ_{max} = 382.4 nm and ε = 4700 M^{-1}) and in the CD bands (at 25 °C, λ = 382.0 nm: $\Delta\varepsilon$ +2.0 M^{-1} cm^{-1}; at 60 °C, λ = 382.0 nm: $\Delta\varepsilon$ −2.6 M^{-1} cm^{-1}), and opens a way to use these polymeric 'nanoshutters' as components in display technology.[33] In the reversible cooperative switching process the helix sense, imine configuration and helical pitch of the polymer does not change. By using Vibrational Circular Dichroism (VCD) and theoretical modelling, the authors could assign the helicity and clarify to some extent the spatial arrangement of the anthracene units (Fig. 2).

In the polymers described above, the introduction of chromophoric units is often difficult due to the demanding reaction conditions required to synthesise these polymers. As a consequence the attachment of chromophores that are able to carry out electron or energy transfer is virtually unexplored. The chromophoric units are mainly used to study interesting phenomena of the polymers themselves, such as the sergeant and soldier effect, the dynamic nature of the helix, helical induction, liquid crystalline behaviour, memory effects and inversion barriers. Potential applications of these helical polymers could be their use as enantioselective catalysts or adsorbents.[37] In order to create systems in which the chromophores are in well-defined positions to generate efficient energy and electron transfer, such as required for photovoltaic devices or field effect transistors, an easy route to prepare such systems is needed. This can be achieved by using polyisocyanides; a class of polymers that have been explored by Nolte, Deming, Clericuzio, Yashima, Takahashi, Amabilino and others over

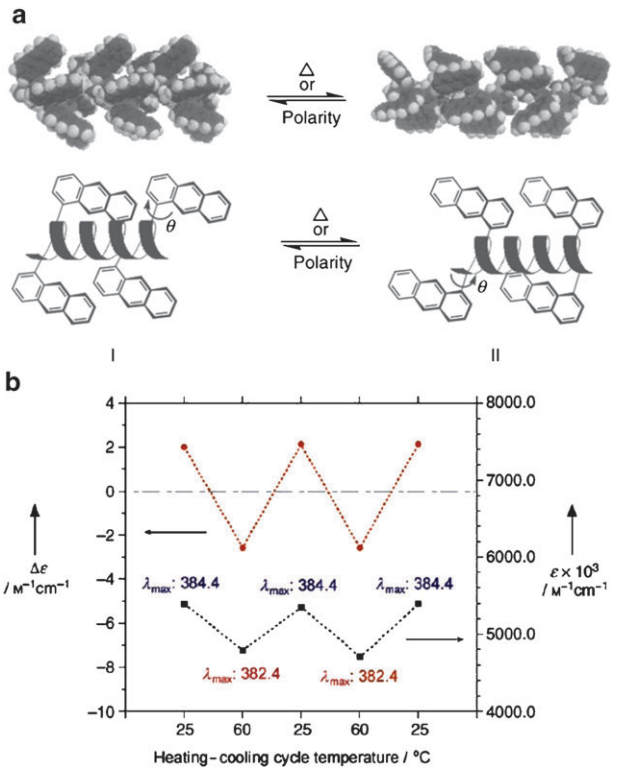

Fig. 2 (a) Theoretical models of the two states that result from the shutter-like motions of the anthracene units of **3** upon the application of heat or solvophobic driving forces. (b) Heating–cooling thermal cycles of **3** in toluene. (*Adapted with permission from ref. 33 Copyright 2005, Wiley-VCH.*)

the last thirty years. Polyisocyanides were the first polymers to be reported to possess a stable helical conformation.[38] The relatively easy preparation of the monomers, the very mild polymerisation conditions and the well-defined structural properties of the resulting polymers have made them very attractive scaffolds on which chromophores can be ordered.[39,40] Due to the specific 4_1 helical nature of these polymers, the side groups are all placed at exact distances and precise positions with respect to one other (Chart 2). This ordering may allow for strong excitonic interactions between the chromophores over large distances, thus enabling the principle of chromophoric scaffolding to be realised. This principle was first successfully demonstrated by Hong and Fox who incorporated aromatic donor and acceptor side arms into homo, di- and tri-block copolymers to create a stiff polymer array for unidirectional electron and energy transfer.[41,42] With the help of fluorescence spectroscopy it was shown that the rigid polyisocyanide backbone was able to spatially define the chromophores and to inhibit the formation of excimers, which is rather surprising since the connection between the polymeric backbone and the aromatic side chains consisted of flexible ethyl linkers. In the block copolymers **4** and **5** (Chart 2) a singlet energy migration was observed at the donor–acceptor interface, which resulted in exciplex formation in the case of **4** and electron transfer at the block interface in the case of **5**. To suppress the formation of exciplexes a tri-block copolymer was developed that contained an intervening pentamethylphenyl block between the respective donor and acceptor blocks of polymer **6** (Chart 2).

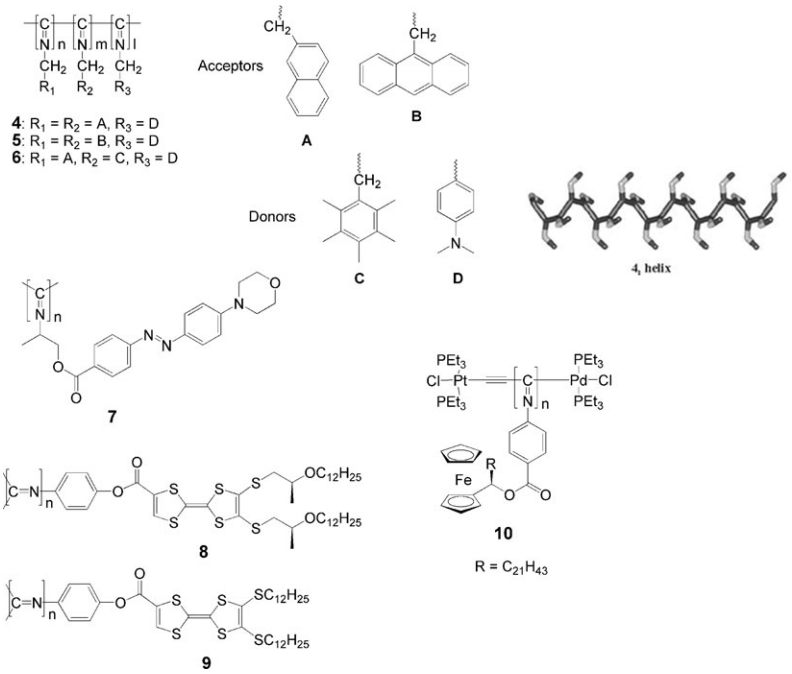

Chart 2 Chemical structures of polymers **4–10** and schematic representation of the 4_1 helical conformation of polyisocyanides.

Transient absorption spectroscopy of the anthracene functionalised polyisocyanide **5** revealed the formation of a radical ion pair with a long-lived lifetime of 1.1 μs. Analogous to the related helical polyisocyanate polymers, polyisocyanides were also decorated with azo dyes (polymer **7**), which acted as non-linear optically (NLO) active groups.[43–45] In solution a first hyperpolarizability exceeding 5000×10^{-30} electrostatic units was measured. Electric field-induced second-harmonic generation studies were conducted and these revealed that the non-linear response of polymer **7** was larger than that of the monomer.[45] When the polymer was studied at the air–water interface by using Langmuir–Blodgett films, a stable second harmonic generation, without the need of poling, was observed.[43,46] This NLO effect is a consequence of the highly defined orientation of the side arm chromophores on the scaffold, which cannot be achieved by the simple assembly of the monomers at the air–water interface.

The group of Amabilino synthesised the challenging (chiral) electroactive polyisocyanides bearing tetrathiafulvalene (TTF) derivatives.[47,48] One such polymer (**8**; Chart 2) was found to possess three extreme univalent states (UVSs) and two very wide mixed-valence states (MVSs), which are fully interconvertible as a result of fully reversible redox processes (Fig. 3). It was shown by CD spectroscopy that the polymer had very different chiroptical properties in comparison to the monomer, which are induced by the stereocentre located more than ~18 Å away from the polyimine backbone. The different redox states of the polymer were investigated by both cyclic voltammetry (CV) and UV-Vis spectroscopy and these studies showed that, by using a rigid scaffold, redox systems can be incorporated in a well-defined manner and hence allow these polymers to be used as multistate redox-switchable organic materials in molecular devices.[48] More recently, the same group has synthesised a related TTF derivatised polyisocyanide **9** (Chart 2) and, based on various spectroscopic techniques,

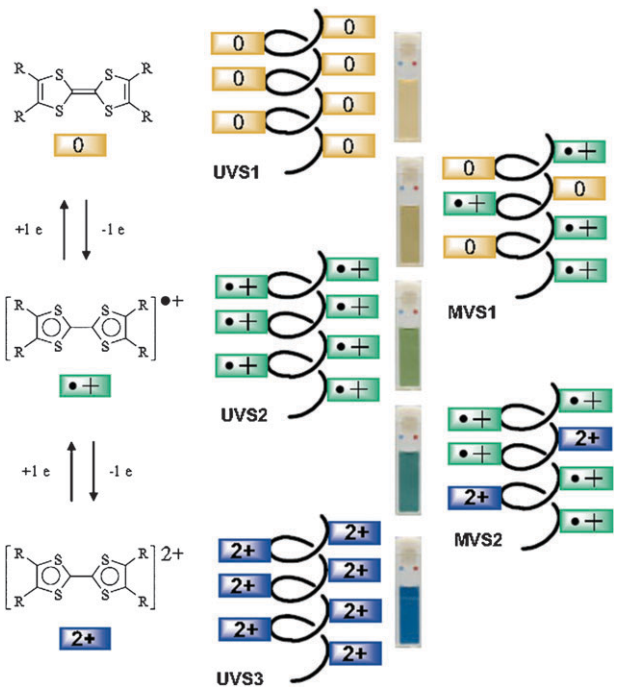

Fig. 3 Schematic representation of the redox properties of the TTF units in the TTF functionalised polyisocyanide showing three univalent states (UVSs) and two mixed-valence states (MVSs). The corresponding colours of the polymer solutions are indicated in red, green and blue. (*Adapted with permission from ref. 48 Copyright 2005, Wiley-VCH.*)

concluded that, due to the precise arrangement of the π-electron-rich units, a charge transfer between the TTF moieties is observed upon oxidation.[47]

Redox active polyisocyanides have also been reported by Takahashi and co-workers,[49] who synthesised a chiral ferrocenyl

isocyanide (monomer of **10**, Chart 2) and polymerised this monomer by using a Pd–Pt μ-ethynediyl dinuclear catalyst, which is especially active for aryl isocyanides.[50] The recorded redox cycles of the polymer **10** were completely reversible with a half-wave potential of approximately 0.6 V. The CD spectrum of the polymer exhibited a strong positive effect at λ = 360 nm, assigned to the n–π* transition of the imine group, and a strong negative one at λ = 250 nm assigned to the π–π* transition of the benzene rings. Upon electrochemical oxidation of the polymer at 1 or 1.5 V, the CD spectrum showed a decrease in the intensity of the positive Cotton effect at λ = 360 nm to 40% of the initial value and the disappearance of the negative Cotton effect at λ = 250 nm. In the UV-Vis spectrum new absorption bands at λ = 240–310 and 620 nm appeared upon oxidation, which were attributed to the ferrocenium chromophore. The CD signal could be restored to the original one by reduction of the polymer at 0.2 V. This switchable behaviour was also observed in the case of a chemical oxidation with $[NO][PF_6]$ and a reduction with $[(C_5Me_5)_2Fe]$, suggesting that upon oxidation the helical backbone is transformed into a disordered structure by the electrostatic repulsion between the ferrocenium ions, yet refolds upon the reduction of these ions. This observation again highlights the advantage of a helical scaffold, which is able to restore high order upon oxidation or reduction.

Due to their versatility and their unique optical properties, numerous synthetic multi-porphyrin arrays have been developed by both covalent or non-covalent procedures[51] to generate materials with a broad range of potential applications.[52] The family of chromophoric polyisocyanides has been extended by the construction of porphyrin appended polyisocyanides, initially reported by the groups of Takahashi[53–57] and Nolte (Chart 3).[58,59] By using a Pd–Pt μ-ethynediyl dinuclear catalyst, the living polymerisation of various porphyrin pendant isocyanides was induced, which resulted in polymers **11–15** with precisely controlled molecular weights (see Fig. 4 for a calculated model of polymer **11**).[53–57] In this way, for instance, a polymer with *ca.* 100 attached porphyrins was obtained. Changing the monomer to catalyst ratio allowed the degree of polymerisation to be varied from 2 to 200, which could be visualised by an increase in the intensity of the band at λ = 400 nm in the UV-Vis absorption spectra of the polymers.

Photophysical studies revealed that the porphyrins in their stacks are excitonically coupled and arranged in a face-to-face manner. It was found that exciton–exciton annihilation rate constants were independent of the length of the polymer, which indicates a fast exciton migration through the stacks. Since the dinuclear metal catalyst also allows the possibility to construct block-copolymers, polymers of type **14** and **15** with various block lengths and with polydispersities of ~1.1 were prepared. The di- and tri-block copolymers contained both free base and zinc substituted porphyrins and displayed an energy transfer from the zinc to the free-base porphyrins with an efficiency of 35% in the case of **15**.[57] The rate constants for the excitation energy transfer process appeared to be the same for different block lengths of the free base and zinc porphyrins, again pointing to a fast exciton migration. In a novel approach Takahashi and co-workers also used the porphyrin as a

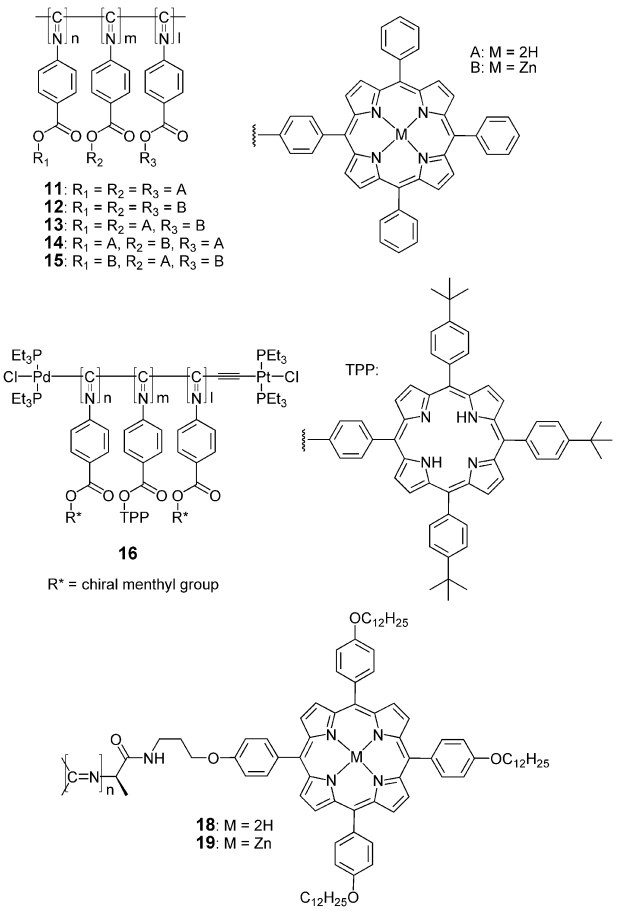

Chart 3 Chemical structures of polymers **11–19**.

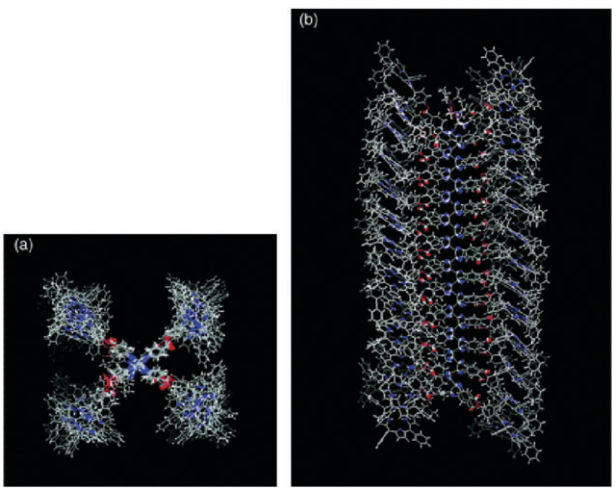

Fig. 4 Top (a) and side view (b) of the energy-minimized structure of **11** (50 units) showing the stacks of porphyrins running parallel to the main chain of the polymer. (*Adapted with permission from ref. 57 Copyright 2004, American Chemical Society.*)

spectator group in order to determine the screw sense of their polymers.[54] Incorporation of achiral porphyrin molecules as a central block in copolymer **16**, where the side blocks consisted of enantiopure menthyl side chains, resulted in a helical polymer with a preferred handedness in which the rigid helical conformation was maintained. Since the polyisocyanide

architecture enforces an extremely short distance between the stacked porphyrin chromophores an exciton coupled bisignate Cotton effect was observed in the Soret band in the CD spectrum. From the sign of this Cotton effect the screw sense of the polymer could be determined using the exciton chirality method.[60–62] In a study published in 1985, Nolte and co-workers investigated the use of polyisocyanides as scaffolds for the grafting of porphyrins onto the polymer backbone to obtain catalytically active polymeric materials. This approach, however, resulted in incomplete coverage of the polymer chain with porphyrins and hence no complete homogenous stack of these molecules was obtained.[58] The discovery of the peptide based polyisocyanides, reported by the Nolte group in 2001,[63] opened a new way to use polyisocyanides as macromolecular scaffolds, since the peptide amide functionalities allowed the side groups to be aligned in one direction. This resulted in a hydrogen bonding network in the side chains of the polymers and hence a dramatic increase in rigidity of the overall structure, making it a better scaffold for the anchoring of chromophoric molecules (Fig. 5).

An additional benefit of these very rigid polymers (persistence length is ~76 nm) is that they can be synthesised with lengths ranging from hundreds of nanometres to several micrometres.[64] The helical porphyrin functionalised polyisocyanides **18** and **19** (Chart 3) were synthesised with average lengths of approximately 100 nm, as determined by Atomic Force Microscopy (AFM). This corresponds to a degree of polymerisation of ~830. The polydispersity of these polymers was ~1.3.[59] The UV-Vis absorption spectra (Fig. 6) of the polymers showed a sharp Soret band at λ = 437 nm, indicative of porphyrin

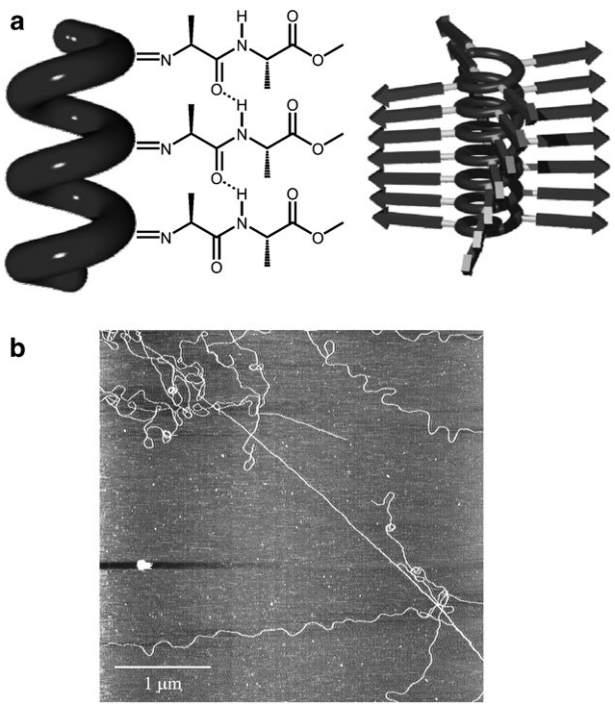

Fig. 5 Schematic drawing of the hydrogen bonding network present in the side arms of a polyisocyanopeptide (a) and an AFM image (b) showing the fibre like structures with lengths up to several micrometres. The arrows in (a) are the peptide chains which form a β-sheet-like architecture running parallel to the polymer helix axis.

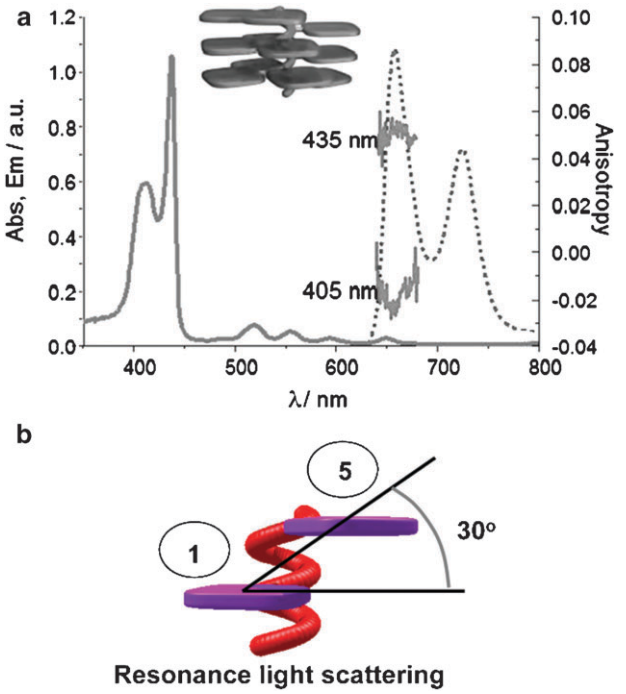

Fig. 6 (a) Absorption (black line), emission (dotted line) and fluorescence anisotropy spectra of **18** in toluene and (b) schematic illustration showing the orientation of the porphyrins 1 and 5 in the polymer with a slip angle of 30°.

molecules arranged as J-aggregates. This band displayed a reversible change upon heating in organic solvents with the intensities of the CD bands of the chromophores decreasing upon warming and increasing upon subsequent cooling; this implies that the porphyrin architecture is a thermodynamic minimum. Resonance light scattering (RLS) experiments revealed that upon excitation the excited state is delocalized over at least 25 porphyrins in one stack, which corresponds to a delocalisation distance of ~100 Å. Depolarised RLS studies revealed that the slip angle β between the first and the fifth porphyrin amounted to 30° (Fig. 6), which results in a helical twist angle of 22° and an overall helical pitch of ~68–71 Å. Fluorescence anisotropy studies were performed to obtain additional information about the orientation of the porphyrins along the polymer scaffold. It was calculated from the anisotropy measurements that the porphyrin moieties are tilted by approximately 25° with respect to the helical axis of the polyisocyanide. The anisotropy measurements, in combination with the RLS studies, revealed an architecture in which the chromophores form a four-fold helter-skelter arrangement along the polymer backbone. The presence of a chiral interaction between monomer n and $(n + 4)$ in this slipped arrangement and between the neighbouring porphyrins n and $(n + 1)$ in the helix could be derived from CD spectroscopy. In the CD spectra intense CD bands were observed, which are reminiscent of the energy transfer process in the natural antenna systems and are ascribed to exciton delocalisation over large distances. Upon the addition of the bifunctional ligand 1,4-diazabicyclo[2.2.2]octane (DABCO) to the zinc porphyrin containing polymer **19** the CD spectrum changed to one that is indicative of a conformation in which the porphyrin stacks

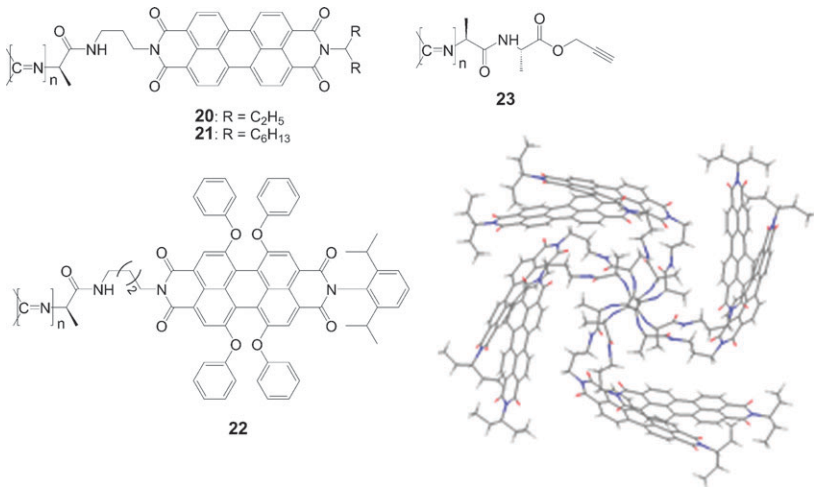

Chart 4 Chemical structures of polymers **20–23** and a top-view of the most probable conformation of the helix of **21** and the relative orientation of the perylene molecules.

possess a helicity opposite to that of the DABCO free polymer. In line with this the infrared and CD spectra of the polyisocyanide backbone remained unaltered by the addition of DABCO.

To further explore the concept of organising pigments on rigid polymer scaffolds, polyisocyanides **20–22** possessing perylenediimides (PDIs) (Chart 4), which are promising chromophores in organic electronic n-type materials, were explored.[65–70] The combination of the hydrogen bonding arrays together with the additional π–π stacking interactions of the perylene side groups resulted in very stable helical polymers.[65–70] Fluorescence spectroscopic studies on **20** showed the presence of a broad, structureless, and red-shifted band in the emission spectrum of the polymer, indicative of an excimer-like species. Fluorescence decay measurements revealed that species with a long lifetime of 19.9 ns were present, further supporting the idea that emission from these polymers occurred through an excimer species. By using a combination of confocal fluorescence microscopy and AFM, it was possible to show that two species were formed in the polymerisation reaction, *i.e.* ill-defined oligomeric and well-defined polymeric species. The first species could not be visualised by AFM since they were too short, and they displayed monomer-like fluorescence. The latter species had a more well-defined rigid structure and could be visualised as independent fibres by AFM. These longer fibres were found to primarily exhibit excimer emission. It could be concluded from a combination of confocal fluorescence spectroscopy and AFM that upon excitation of these longer rods, the emission is moved along the isoelectronic perylene arrays and became quenched at perylene dimer sites, which resulted in excimer emission. These dimer sites can be fixed defects in the polymer or dynamic excimers that are formed throughout the polymer.

Because polymer **20** was poorly soluble in organic solvents, polymer **21**, which contains long alkyl tails and hence improved solubility, was synthesised.[70] Extensive dynamic and molecular modelling studies, combined with spectroscopic studies, indicated that **21** is an ideal polymer system for electron and energy transport. This hypothesis was further strengthened by transient absorption spectroscopy studies, which indicated extremely rapid exciton migration rates and high charge densities in polymer **21**. The modelled structure as depicted in Chart 4 shows the calculated PDI ordering, which accounts for all the physical properties (UV-Vis and CD) observed.

The electronic transport properties of the polymer stacks were examined in thin-film transistors and the experiments revealed carrier mobilities of the order of 10^{-3} cm^2 V^{-1} s^{-1} at 350 K, which were found to be limited by inter-chain transport processes. This mobility value is intermediate between the values observed for amorphous spin-coated films of perylene and single-crystal perylenes.[68] Photovoltaic cells with an active layer of **21** as the electron acceptor and either poly-3-hexylthiophene (P3HT)[67,69] or poly(9,9′-dioctylfluorene-co-bis-*N*,*N*′-(4-butylphenyl)-bis-*N*,*N*′-phenyl-1,4-phenyl-diamine) (PFB)/poly(9,9-dioctylfluorene-co-benzothiadiazole) (F8BT)[69] as electron donor were prepared and, although the overall efficiency was rather low (∼0.2%), a 20-fold improved power output compared to a cell with an active layer of a monomeric perylene homologue and P3HT was observed. In order to visualize the relationship between the architecture and the photovoltaic efficiency, AFM and Kelvin Probe Force Microscopy (KPFM) measurements were carried out on polymer films (Fig. 7) by the group of Samori.[67] This allowed the direct visualization of the photovoltaic activity occurring in polymeric bundles of electron-accepting PDI wires and bundles of electron-donating P3HT chains with true nanoscale spatial resolution. It was evident from these AFM/KPFM and spectroscopic studies that the well-defined polyisocyanide chromophoric system has promising characteristics for applications; it enhances the lifetime of the separated state and is more efficient than monomeric perylene materials in a photovoltaic device.

The addition of bulky phenoxy substituents to the perylene bay area leads to a sterically hindered polyisocyanide (see **22**; Chart 4) and limited π–π stacking of the PDIs. The low quantum yield (3%) of the polymer is in line with H-aggregated PDI units. In contrast to the behaviour of **20** and **21**, the emission spectrum of **22** gave no evidence for the formation of excimers, which is consistent with the conclusion that the steric bulk seems to prevent the formation of excimeric pairs in **22**.

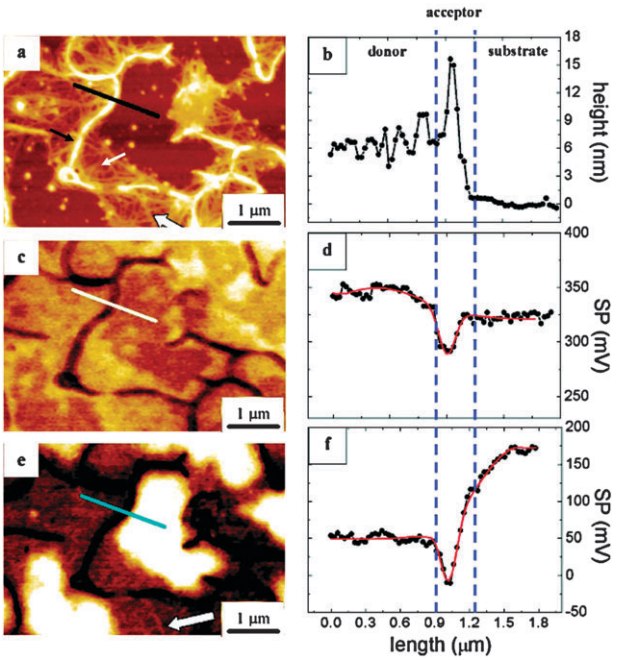

Fig. 7 (a) AFM image of a thin blend of **21** and P3HT deposited on silicon. (c, e) KPFM data of thin films of **21** and P3HT and surface potential images of the same area as in (a), without (c) and with (e) illumination by white light ($\sim$60 mW cm^{-2}). An overall negative potential shift upon illumination is visible. (b, d, f) Measured (black lines) and simulated (red lines) profiles obtained by tracing the arbitrary lines ((a) black, (c) white and (e) light blue) in the corresponding images (a), (c) and (e). (*Adapted with permission from ref. 67 Copyright 2008, American Chemical Society.*)

Although polymers **20–22** are promising candidates for electron transfer their syntheses are extremely demanding. A more modular approach to prepare such polymers, based on the post-modification of a well-defined polyisocyanide scaffold was therefore developed. Polymeric scaffold **23** (Chart 4), with side arms containing two alanine groups and a terminal acetylene functionality, was synthesised. This compound can be easily modified by reacting it with azides using the well-established click-chemistry approach.[71,72] The wide variety of azides available allows one to access a vast array of functionalised polymers with varying properties.

The clicking of ethylene glycol azides to polymer scaffold **23** was found to result in the formation of water-soluble polymers. The co-clicking of the scaffold with the same azide in conjunction with a perylene azide gave, for the first time, chromophoric water-soluble polyisocyanopeptides, which exhibited the same CD spectrum in water as in dichloromethane. By the use of two chromophoric azides, a coumarin dye and a perylene dye, random copolymers were formed in which the absorption and emission from both chromophores were present. Furthermore, interaction between the chromophores was observed, evidenced by a quenched and blue-shifted emission of the coumarin molecules that are in close proximity to a perylene molecule. This shows that two different chromophores can now be readily incorporated into the polymers and opens the way to polymeric materials with a wide range of optical properties.

The above presented approach, in which a rigid polymer chain is used as a scaffold in order to control the position of dye molecules, is a very versatile one. The mechanical properties of the polymers, that is their rigidity on the nanometre scale, the flexibility of the linker and the stacking of the dye molecules, can all be adjusted by chemical modification. The ability to orient chromophores in space into a more efficient energy and electron transfer geometry, which cannot so easily be achieved by self-assembly, offers considerable opportunities for materials with improved mechanical and opto-electronic properties.

3. Carbon nanotubes and related structures

An alternative way to arrange chromophores is to employ a carbon nanotube (CNT) as a scaffold to which chromophores can be attached. Since CNTs possess unique properties, numerous modifications have been developed in order to improve their solubility and electronic properties. CNTs may also find applications for the transport of biological molecules.[73–76] The ability to attach chromophores to CNTs would allow for their visualisation and possible tracking of the movement of biomacromolecules. The study of CNTs in combination with chromophores has, however, been primarily focussed on the grafting of chromophores onto CNTs for photo-induced electron transfer. In general, two strategies have been employed, *i.e.* covalent and non-covalent (supramolecular) functionalisation of CNTs. It is important to note that, due to the method of preparation, CNTs have been randomly decorated and hence in a less controlled manner in contrast to, for example, viruses or polymers, which are built up from chromophoric monomers that are subsequently self-assembled or polymerised. The covalent approach to chromophoric functionalised CNTs was utilized by Sun and co-workers.[77] They synthesised porphyrin decorated single-walled CNTs (SWNT) with the porphyrin molecules covalently attached to the nanotubes with either a short (CH_2) or a long (C_6H_{12}) linker. From fluorescence studies it became evident that for the long linking species the fluorescence is suppressed, presumably due to the stacking of the porphyrin units because the spacer was flexible. The fluorescence of the compounds with a short spacer revealed that the photo excited state properties of the chromophores remained unaffected, that is no quenching of the fluorescence was observed. In related work, porphyrin molecules were directly linked to the CNT through an ester linkage (Fig. 8).[78] By using thermogravimetric analysis (TGA) a grafting density ranging from 8–22% was found to be present. Upon excitation at λ_{exc} = 550 nm of the porphyrin-SWNT hybrid the emission was almost fully quenched with the energy being channelled into the SWNT. No intermolecular electron transfer between the porphyrins was reported.

The covalent attachment of phthalocyanines to CNTs resulted in stable assemblies, for which steady-state and time resolved fluorescence spectroscopy studies indicated that a strong photophysical interaction was present between the chromophores and the CNTs.[79] Following on this success, novel phthalocyanine-CNT complexes were prepared utilising the click chemistry protocol.[80] These complexes were tested for their photovoltaic properties and internal photoconversion

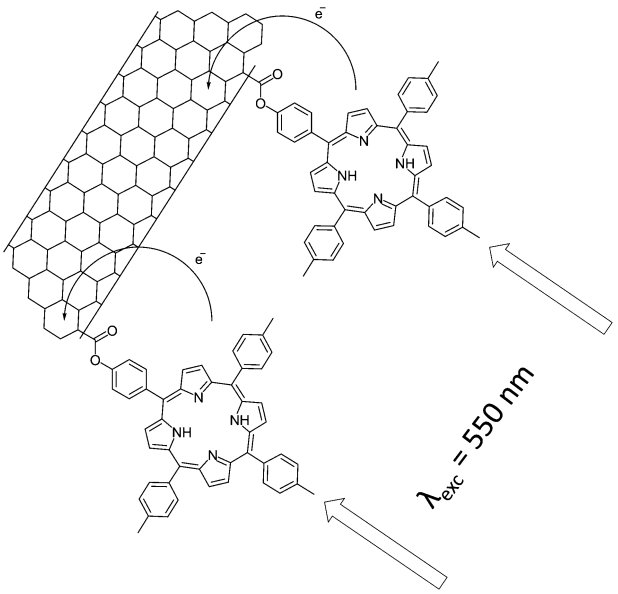

Fig. 8 Porphyrins linked to CNTs through an ester linkage leading to almost complete photoinduced electron transfer from the porphyrin to the CNT.

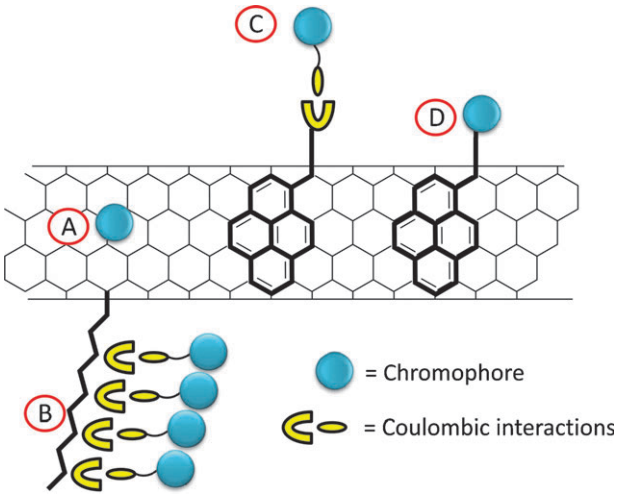

Fig. 9 Schematic drawings of the four approaches developed to construct chromophoric CNTs complexes.

efficiencies (ICPE) up to 17.3% could be reached, which suggests a considerable potential for such systems.

Another class of chromophores that could serve as donor materials in CNT complexes are TTF molecules.[81] The SWNTs have been modified with carboxylic acid groups, followed by 1-(3-dimethylaminopropyl)-3-ethylcarbodiimide hydrochloride (EDC) coupling to an alcohol functionalised TTF to give the nano-hybrid materials. Spin-coated solutions on silicon wafers revealed thin bundles as well as aggregates of tubes. Furthermore, by changing the spacer between the TTF and the CNT or by extending the π-system of the TTF the charge separation and the charge recombination could be controlled. Recently, also graphene, a very promising candidate in materials science, has been used as a support to arrange porphyrin molecules.[82] From detailed infrared (IR) and UV-Vis spectroscopy studies, as well as Transmission Electron Microscopy (TEM) studies, it could be concluded that the used amino porphyrins were covalently linked to the graphene oxide through an amide bond. It appeared that the fluorescence of the porphyrin molecules in these donor–acceptor nano-hybrids was quenched due to a possible electron-transfer process.

Although the covalent approach for the preparation of these materials is very versatile it may lead to a disruption of the π-system of the CNTs and hence in partial loss of electronic and structural properties. For this reason non-covalent procedures, which, in principle, are more simple to apply and rely upon Van der Waals, π–π stacking and/or Coulombic interactions were also investigated. In general, four approaches have been used to create chromophoric carbon nanotubes in which the chromophores are non-covalently linked to the CNT (Fig. 9). These are based on (i) simple non-covalent interactions between the chromophore and the CNT (A), (ii) a charged polymer that is covalently attached to the CNT allowing multiple Coulombic interactions with an oppositely charged chromophore (most often a porphyrin) (B), (iii) charged pyrene derivatives that have favourable π–π stacking interactions with the CNT and also interact through Coulombic interactions with an oppositely charged chromophore (C) and (iv) a chromophore that is directly attached to a pyrene molecule, which interacts with the CNT (D). In all cases supramolecular assemblies are created where the donor and the acceptor are in close contact leading to interesting properties. In these approaches there is, however, no direct control over the positioning of the chromophores in the hybrid since the attachment to the CNT occurs at random. It is of interest to note that the rigid structure of the CNT, in most cases, is not used as a template to increase communication between the chromophores but to realize strong interactions between these chromophores and the CNTs.

Porphyrins[83–90] and phthalocyanines[91] are the most frequently used dyes to decorate CNTs (Fig. 9, approach A). Early work by Nakashima[83] and Sun[84] reported the generation of stable porphyrin–nanotube hybrids when there was an excess of porphyrin molecules in solution. Removal of the excess porphyrin resulted in precipitation of the nanotubes, which indicates that dissociation of the complex occurs rapidly. Without the complete removal of the excess porphyrin from the porphyrin–nanotube hybrid suspension, detailed photophysical studies could be carried out and these revealed charge transfer features that are persistent on the time scale of hundreds of nanoseconds.[92] The interaction between the porphyrin and the CNT could be enhanced by using conjugated porphyrin polymers[85] or by applying polymer wrapping.[86,87] Kamat and co-workers used CNTs to order protonated porphyrins in the form of J- and H-aggregates.[88] It was demonstrated with the help of TEM that, in the presence of a strong acid, the hybrid complexes assembled into large rod-like structures (Fig. 10a and b) in which the porphyrins were randomly distributed over the CNT. In the absence of a strong acid, the interaction was weaker and clusters of the protonated porphyrins were formed (Fig. 10c). This striking difference is attributed to the strong intermolecular interactions that occur between porphyrin moieties and/or ordered aggregation effects in the protonated form.

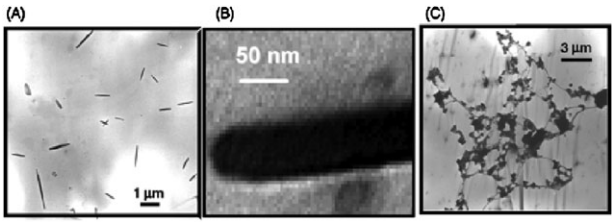

Fig. 10 (a, b) TEM images of the rod-like CNT–porphyrin hybrid complexes that are formed in acidified THF. (c) TEM image of the CNT–porphyrin adducts formed in THF without acid present revealing no clear, assembled structures. (*Adapted with permission from ref. 88 Copyright 2005, American Chemical Society.*)

Water-soluble porphyrin–CNT complexes have also been developed, which allowed the alignment of nanotubes on polydimethylsiloxane (PDMS) surfaces and the subsequent transfer of these objects to silicon substrates by stamping. Despite the presence of large areas of aggregated porphyrins on the silicon substrate, multiple CNTs aligned parallel to each other were obtained.[93] An extensive study into the multiple and complex interactions that are present in non-covalently linked porphyrin–nanotube complexes[89,90,94,95] and in TTF–nanotube complexes[96,97] (as a complementary study to their earlier work in this area[81]) has been published by Guldi, Prato and co-workers.

A water soluble polymer, *i.e.* poly-[(vinylbenzyl)trimethylammonium chloride] ($PVBTA^{n+}$), has been used in combination with CNTs as a positively charged scaffold to align negatively charged porphyrin molecules through electrostatic interactions (Fig. 9, approach B).[90] A similar approach based on negatively charged CNTs and positively charged porphyrin molecules has also been reported.[94] The hybrid complex was readily soluble in water and was found to be stable for months without any observable precipitation. Photoexcitation of the complex in solution resulted in the fast generation of radical ion pairs (*i.e.* 0.15 ns) that had very long lifetimes (2.2 μs). Photocurrent measurements gave monochromatic internal photoconversion efficiencies (ICPE) up to 9.9%. Supramolecular pyrene-porphyrin CNT complexes were prepared by using a combination of electronic and π–π interactions (Fig. 9, approach C).[91,92] Detailed photophysical studies on these complexes revealed that long lived radical ion pairs were formed as a product of the rapid excited-state deactivation of the porphyrin. These studies have given an interesting insight into the processes involved, which is important for the application of these nano-hybrid materials in electronic devices. The same authors have also described a hybrid complex in which the chromophores were directly attached to the pyrene units (Fig. 9, approach D). To this end, a TTF molecule was linked to a pyrene with a flexible linker allowing for optimised interactions with the outer surface of the CNT, leaving the latter structure intact.[91] A ratio of 1 : 750, *i.e.* a single pyrene-TTF unit per 750 carbon atoms of the CNT was estimated to be present in the final complex, as concluded from Thermogravimetric Analysis (TGA). Due to the close distance between the TTF molecules and the CNT, very fast electron transfer (on the nanosecond scale) between these species was observed. Recently, these investigations have been extended to a series of single-walled and multi-walled CNTs.[92] From these studies it was apparent that stable charge-separated states are formed only in the case of multi-walled CNTs as compared to single-walled CNTs, where only short lifetimes were found. This might be explained by a stabilisation of the excited state species in the former cases as a result of the presence of a large number of tubes in the multi-walled CNTs.

Closely related to the family of CNTs are the carbon nanohorns (CNHs).[98] Carbon nanohorns are spherical aggregates typically composed of thousands of carbon nanotubes of about 2–5 nm in diameter and 30–50 nm in length. Their characteristic features include a conical end on one side of the tubular structure, a high porosity and a large (rough) surface area. The aggregation of CNHs leads to the formation of dahlia-flower-like superstructures. Although the use of CNHs as scaffolds for chromophores has not been investigated to the extent it is in the case of CNTs, some examples of porphyrin CNH nano-hybrids have been recently reported. Using approach C (Fig. 9), Ito and co-workers were able to prepare TTF chromophoric nano-hybrids by exploiting the electronic and π–π interactions between the CNH, the positively charged pyrene molecules and the negatively charged TTFs.[99] A comprehensive spectroscopic characterisation, which offered a schematic overview of all the processes taking place in the hybrid, was carried out. These studies indicated an electron transfer process between the TTF units and the CNHs as also reported for the TTF-CNT hybrids.[91] As with CNTs, CNHs could also be decorated with porphyrins by three different routes. These included (i) the simple attachment of the porphyrin to the CNH by direct π–π interactions,[100] (ii) the covalent attachment of the porphyrin to the CNH with an amide bond (see Fig. 11 for the molecular structure and a representative high-resolution TEM image),[101,102] and (iii) the use of ethylene glycol spacers that are covalently linked to the CNHs.[103] In all cases the CNH hybrids were analyzed in detail generating interesting information about the formation of charged separated states, electron transfer and hybrid stability. This information is required for further optimisation of the structures in the case of application in organic devices. Recently, a porphyrin CNH hybrid was used to fabricate a cancer phototherapy system, which highlights the fact that these chromophoric carbon nanostructures are very useful for practical applications.[104]

In summary, CNTs, being one of the stiffest compounds known to date, are attractive scaffolds for the immobilisation of chromophores. Although a high level of molecular control is not always achieved, these nanotubes offer a versatile platform for the construction of interesting donor–acceptor materials. In recent years, the assembly and the structural and photophysical properties of the chromophore-CNT hybrids have been extensively studied and their unique properties will open the way for utilisation in future organic devices.[105]

4. Nucleic acid based architectures

DNA is used by nature to encode information needed for the construction of living organisms. For chemists, DNA constitutes a unique programmable scaffold that holds great promise in numerous areas of nanotechnology.[106] Its key characteristics are:

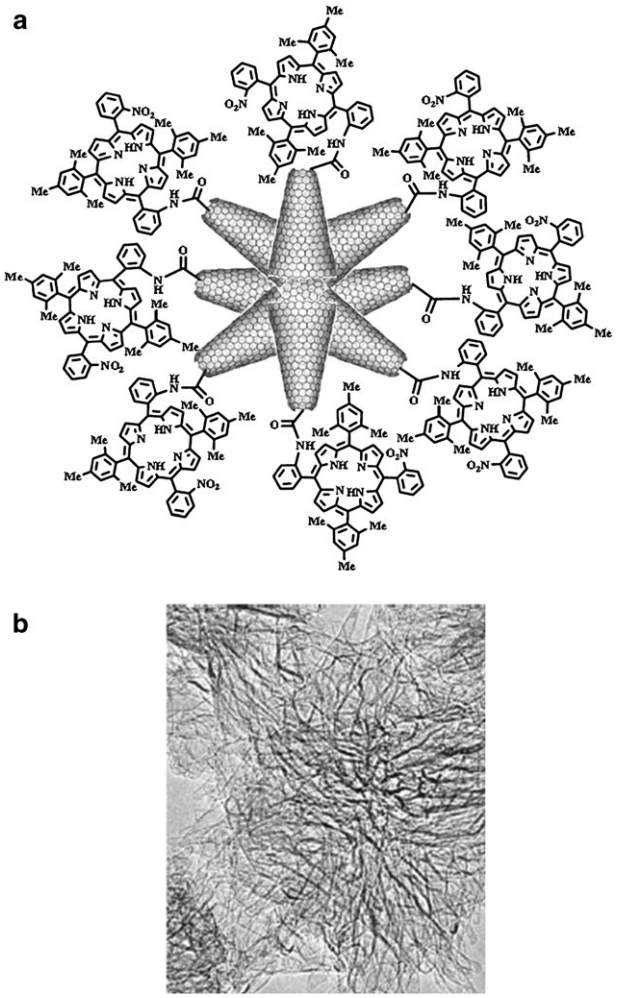

Fig. 11 (a) Schematic depiction and (b) a high-resolution TEM image of the structure of a porphyrin CNH nano-hybrid. (*Adapted with permission from ref. 102 Copyright 2007, Wiley-VCH.*)

(i) the presence of two complementary strands that can be reversibly assembled and disassembled; (ii) the fact that it is chiral (helical) and (iii) very rigid (persistence length of $\sim$50 nm), with an ideal distance between two base pairs for the stacking of chromophores (3.3 Å in the B-form); (iv) the possibility to synthesise it by automated procedures, thereby allowing site specific modification; (v) the possibility to assemble it into complex 3D nano-structures and into nano-devices.

Due to these attractive properties DNA has been receiving increased attention as a scaffold for the precise arrangement of chromophores. In this section, we will highlight recent examples of DNA based multi-chromophoric assemblies which display new properties arising from the electronic communication between chromophores.[107,108] The supramolecular organisation of chromophores as a result of intercalation between DNA base pairs will not be reviewed here.

Two main approaches have been used to organise chromophores on DNA. They can be denoted as "internal stacking" and "outside stacking" (Fig. 12). In the first approach, the Watson–Crick base pairing is partly suppressed since either the base or the sugar part is substituted by the chromophore (Fig. 12). The stability of the duplex is then provided by the base pairing at the unmodified sites and the contribution by the internal stacking of the introduced hydrophobic chromophores. In some cases, this internal arrangement constitutes a recognition motif that, in some way, can be viewed as an artificial base pairing (*vide infra*). In the second approach, the full Watson–Crick base pairing of the functionalised nucleotides is maintained, while also the base or the sugar is modified (Fig. 12). The chromophores are thus tethered either to the 5 position of the pyrimidine ring or to the 7 position of the deazapurine ring of DNA, to maintain the *anti* conformation of the modified nucleoside. Another possibility to generate arrays of chromophores is to use an RNA scaffold, since the 2′ position of the sugar can be readily derivatised without modifying the base, or to use Lock Nucleic Acids (LNA) by taking advantage of the 2′-4′ bridging unit as an anchoring site for a chromophore. This second approach has led to an "outside stacking" of the chromophores (Fig. 12), which can further interact with the hydrophobic grooves generated by the "intact" internal stacking of the base pairs. In both approaches, adjacent chromophores can be brought close to one another and the distance between two base pairs (and thus between two anchoring sites) is optimal for physical communication between the chromophores. In this section we will mainly focus on chromophoric scaffolding using DNA.

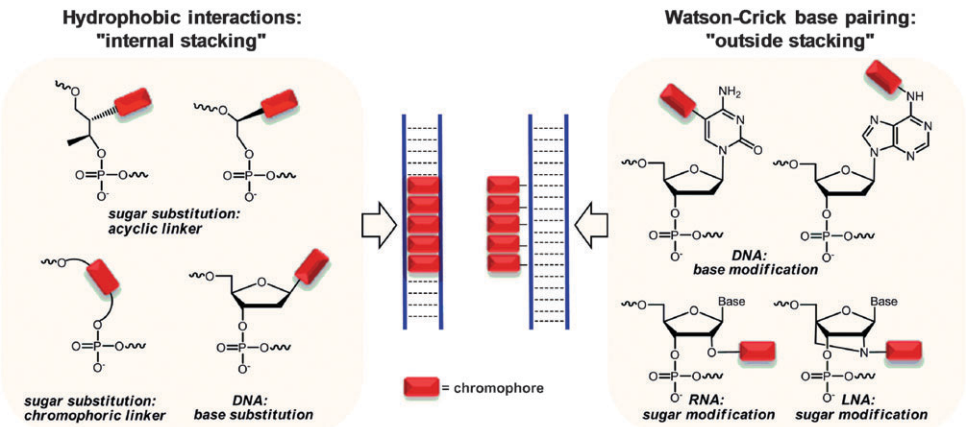

Fig. 12 Strategies for the construction of chromophoric assemblies with the help of DNA based scaffolds.

Related work with RNA and LNA has been recently highlighted and will not be discussed here.[108]

First approach: internal stacking

Inspired by the structure of the DNA skeleton, the group of Kool has developed a new class of assembled fluorescent molecules, the so-called 'fluorosides'. They consist of short oligomers (generally tetramers) of C-nucleosides to which individual chromophores are grafted. The replacement of the DNA bases by flat aromatic (hydrophobic) molecules allows them to stack but also provides water solubility, thereby mimicking single-stranded DNA. The close interaction of the chromophores is of interest for energy transfer and the possibility to easily tune the sequence of the chromophores (with a DNA synthesiser) allowed Kool and co-workers to synthesise libraries of oligofluorosides with unique properties.[109] As displayed in Fig. 13a, a 256-member library composed of all combinations of fluorosides D, E, Y and Q was grown from PEG-polystyrene beads. The fluorescent properties of the tetra-fluorosides were found to be different from those of the individual chromophores, that is large Stokes shifts and tuned absorption and emission properties were often observed. In addition, the emission was sequence dependent such that at least 50 different colours could be distinguished by the naked eye. A study conducted with fluorosides made of only two chromophores but with different sequences revealed the importance of the neighbouring interaction; the fluorophore sequence in such oligomers turned out to be as important as the fluorophore composition in determining the fluorescence properties.[110,111] The large Stokes shifts of the oligofluorosides and their increasing brightness with increasing substitution make them particularly suited for biochemical and biophysical applications.[112] This work was extended to larger libraries (11^4 = 14 641 members) for the discovery by rapid combinatorial screening of sensors that change colour on light exposure.[113] From this library, three tetrafluorosides were selected and further studied. Upon light exposure a blue shift in the fluorescence was observed, probably caused by the selective reaction of one chromophore with oxygen (Fig. 13b). This might result in the loss of the initial excimer fluorescence and the emergence of monomer emission at shorter wavelengths. The clear separation of starting and final emission colours in these tetrafluorosides opens the possibility to measure light exposure over time.

The various oligomers could be simultaneously excited with a long wavelength UV light (*i.e.*, 340–380 nm) to produce multiple emission colours. This is of particular interest in connection with the simultaneous tracking of more than one species by colour and maybe useful for the visualisation of species in moving systems where classical fluorophores fail. For instance, a set of 23 oligodeoxyfluorosides (ODFs) was prepared from a library with emission maxima ranging from 376 to 633 nm, thus yielding apparent colours from violet to red, all of which can be visualized directly (Fig. 13c). Preliminary *in vitro* and *in vivo* experiments showed that the ODFs could penetrate the cellular membrane and tissues, were biostable and displayed no apparent toxicity in human tumor (HeLa) cells and live zebrafish embryos.[114] More importantly, multispectral imaging could be successfully carried out with a set of four dyes in real time in a dynamic system (living embryos) without the need for reconstructing of separated colour images (Fig. 13d).

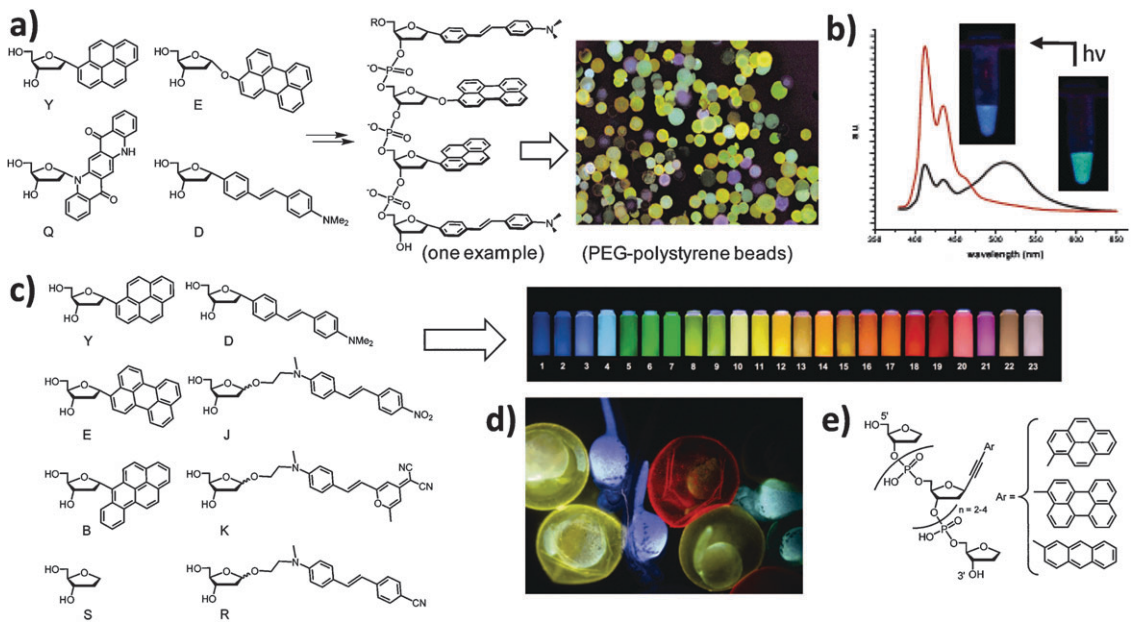

Fig. 13 (a) Construction of a 256-member library of tetrafluorosides from four different fluorosides leading to a wide range of colours at a single excitation wavelength; (b) application to the development of a light sensitive sensor; (c) various fluoroside monomers used for the selection of a set of 23 oligofluorosides displaying colours that cover the complete visible spectrum and (d) the use of four oligofluorosides (blue, cyan, yellow and red emitting) in the simultaneous observation of differently labelled live zebrafish embryos (the dyes were separately incubated with embryos; real image at 48 h post-fertilisation with excitation at 354 nm); (e) related fluorescent oligomers based on alkynyl C-nucleosides developed by Inouye and co-workers. (*Adapted with permission from ref. 109, 113 and 114 Copyright 2002, 2004 and 2009, American Chemical Society.*)

In a similar approach, Inouye and co-workers synthesised analogous fluorosides starting from pyrene, perylene and anthracene residues connected to the furanoside through an acetylene linker. The anomeric configuration in these oligomers was exclusively β (Fig. 13e).[115] This latter feature was required in order to investigate in detail the photophysical properties of these fluorescent oligomers. As in the Kool system, physical and electronic interactions were observed between the chromophores and the predominant excimer fluorescence was found to originate not only from homo-oligomers but also from hetero-oligomers.

In the search for non-natural, non-hydrogen bonded hydrophobic base pairs, which could be of potential interest in expanding the genetic alphabet, Leumann and co-workers connected biphenyl (Bph) and bipyridyl (Bpy) residues to C-nucleosides (Fig. 14a). As a result of inter-strand stacking of their distal rings, two Bpy C-nucleoside residues could recognise each other within a DNA duplex with an affinity equal to that of a G–C base pair.[116] When a number of these planar hydrophobic molecules were placed on both strands in the middle of a duplex oligodeoxynucleotide (ODN), they were found to form a zipper-like arrangement inside the duplex without altering the B-DNA conformation of the double helix (Fig. 14a).[117] In the case of Bph homo-interactions, a stabilisation of 3.0–4.4 Kcal per additional Bph pair was measured. This artificial recognition motif opens interesting perspectives for instance in connection with the study of donor–acceptor systems (*vide infra*), the development of binary recognition codes and the realisation of charge transport.

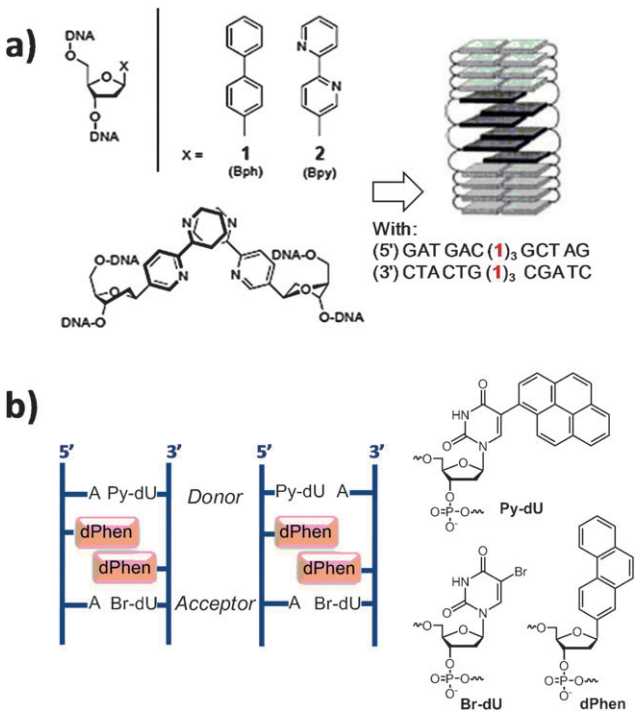

Fig. 14 (a) The two artificial hydrophobic base pairs studied by Leumann and their stacking mode (left) and the representation of the inter-strand zipper array when multiple Bph residues are introduced in the middle of a DNA duplex (right) (*Adapted with permission from ref. 117 Copyright 2003, Wiley-VCH*); (b) the system used by Leumann to study electron transfer through an interstrand phenanthrenyl pair.

Using this artificial base pairing system, the group of Leumann has also investigated electron transfer through a stacked phenanthrenyl pair in DNA (Fig. 14b).[118] Their system was made of 5-(pyren-1-yl)uridine (Py-dU) as a photoinducible electron donor and 5-bromouridine (Br-dU) as an electron acceptor, which also acts as a reporter molecule. The donor and acceptor molecules were separated by an interstrand stack of two phenanthrenyl-C-nucleosides. The overall processes were monitored by quantifying strand cleavage at the level of 5-bromouridine upon illumination using polyacrylamide gel electrophoresis (PAGE) experiments. The authors concluded that electron transfer was effective through the phenanthrenyl stack, but seven times less efficient than in the situation where the phenanthrenes were absent. This was explained by assuming that the electron transfer from the excited pyrene to the phenanthrene was endergonic and proceeded by a superexchange mechanism, whereas electron transfer to a thymine was exergonic and followed the known hopping mechanism. This result, however, is only a proof of principle and further modifications of the phenanthrenyl stack might lead to an improvement in the efficiency.[119]

Another strategy based on sugar substitution, was investigated by the groups of Asanuma,[120–125] Wagenknecht[126–128] and Haner.[129–135] Asanuma and co-workers developed an acyclic linker based on D- or L-threoninol for the incorporation of dyes, such as Methyl Red and Naphthyl Red, into DNA (Fig. 15a). In a first study, up to six dyes were introduced sequentially on an 18 mer strand (Fig. 15bI).[120] In the single strand state, hypsochromicity with a narrowing of the absorption maximum, which increased with the number of incorporated dyes, was observed, indicating the formation of *H** aggregates. This cluster of dyes was, however, only stable in the single stranded form. Upon addition of the complementary strand incorporating an acyclic propanol derivative linker, a new type of aggregate was obtained, as evidenced by a red shift in the absorption maximum along with a broadening of the band. Interestingly, the reversible thermal denaturation/hybridisation of the duplex allowed the switching from one aggregate to the other. Since this strategy was not suited for the modification of a duplex DNA, the dyes were placed in alternating positions on both strands of the duplex, facing the acyclic linker.[121] UV-Vis and CD spectroscopy evidenced the formation of *H* aggregates with hetero- (Methyl Red/Naphthyl Red) and homo-combinations (Methyl Red/Methyl Red or Naphthyl Red/Naphthyl Red) of dyes due to the interstrand stacking of the dyes in a face to face manner (Fig. 15bII and III). It is noteworthy that the new absorption band in the case of the hetero *H* aggregates originated from exciton coupling among the chromophores, which is a rarely reported situation. NMR studies confirmed that the Methyl Red dyes of complementary strands were axially stacked and antiparallel to each other.[122] CD spectroscopy revealed that in the case of the D-threoninol linker the dyes were arranged in a right-handed helix as in the B-form of DNA whereas in the case of the L stereoisomer a less pronounced helix form was obtained. In addition, the duplex structure was found to be

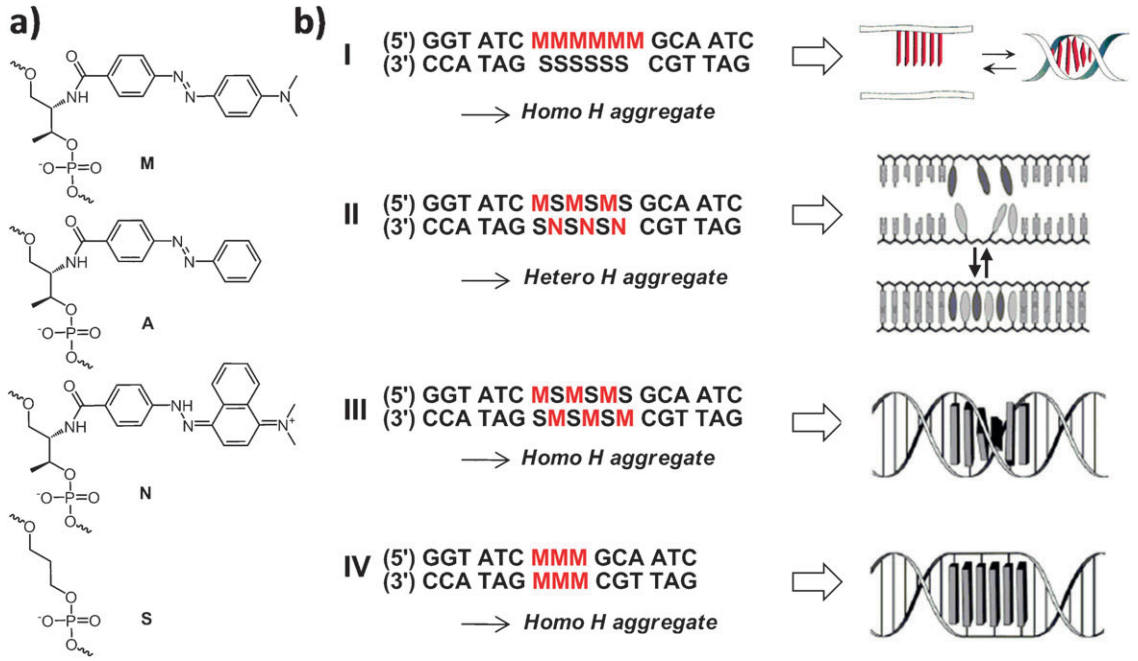

Fig. 15 (a) Structures of the diazo dyes based on an acyclic D-threoninol linker used by Asanuma (*Adapted with permission from ref. 120 Copyright 2003, American Chemical Society*); (b) examples of duplexes modified with dyes and representation of their stacking modes. (*Partially adapted with permission from ref. 121 Copyright 2004, Wiley-VCH.*) (Fig. 15b (*partially*) *reproduced by permission of the Royal Society of Chemistry, ref. 123.*)

stabilised in the case of homo-clustering if no acyclic linker was facing the dyes (thus leading to pseudo base pairs, Fig. 15bIV). This generated an unwound cluster of stacked chromophores resembling a ladder-like structure and with stronger exciton coupling interactions.[123] These differences in dye clustering nicely illustrate how a DNA-inspired scaffold can be used to fine tune chromophore–chromophore interactions. In different work, the reversible photo-switching mode between the *cis* and *trans* form of a diazo dye was used to construct a photoresponsive molecular tweezer.[125]

Wagenknecht and co-workers used (*S*)-aminopropan-2,3-diol as an acyclic linker in the phosphodiester backbone to introduce perylene diimide units (PDI) into a DNA duplex (P, Fig. 16a).[126,127] The (*S*) configuration of the linker was chosen in order to mimic the stereochemical situation at the 3′-position of the natural 2′-deoxyribofuranoside and the linker was tethered to one of the imide functions of the PDI. When placed on both complementary strands, an interstrand PDI dimer was found to stabilise the duplex by 2.4 °C, which is rather unusual for such a modification with a flexible acyclic linker. The interstrand stacking of the PDIs, which can be seen as an artificial DNA base substitution, give rise to a typical excimer fluorescence signal and could be used as a readout for the pairing interaction. Interestingly, when two PDI chromophores were introduced on the same strand around a questionable site where a base mismatch or deletion could be present (Fig. 16a), no excimer fluorescence was observed in the case of a correct base pairing. In contrast, almost exclusively excimer fluorescence was detected in the case of a wrong base pairing. This allowed the determination of the amount of matched counter strands in a mixture of counter strands that differ only in a single base, which is of obvious interest for diagnostic applications.

These studies were extended to systems with up to six chromophores.[128] Interstrand alternating sequences of PDI and thymine or abasic sites were designed to obtain a zipper like arrangement of the PDIs with characteristic excimer fluorescence (Fig. 16b). The compounds displayed exciton coupled CD signals indicative of a helical arrangement of the stacked PDI units in the duplex. The helix sense was found to be directed by the DNA scaffold if no sterically demanding thymine groups were present (Fig. 16b, X = S). In contrast, in the presence of thymine (Fig. 16b, X = T) the PDI aggregates were forced to adopt a different stacking mode, with the angles between the chromophores being alternating 35–45° (left) and 85–95° (right) (see the model in Fig. 16b). This work again highlights the flexibility of the "DNA approach" in respect to tuning chromophoric interactions.

A different approach was followed by the group of Haner, who prepared compounds in which the chromophore itself, *i.e.* phenanthrenyl group, was the linker between two phosphodiester functions (Fig. 17a). The introduction of up to 14 of these residues, in the middle and on both strands of a duplex ODN, could be done successfully.[129] Apart from the stabilising effect of the flanking nucleobases, stabilisation also came from interstrand stacking interactions of the phenanthrenyl residues from opposite strands leading to only a slight decrease in stability of 1.2 °C per artificial base pair modification. Modelling of a hybrid with seven phenanthrene base pairs revealed a significant lengthening of the DNA duplex in comparison to the unmodified duplex, with the same overall number of residues. According to CD measurements the B-DNA structure was not destroyed (Fig. 17a). It is noteworthy that the interstrand clustering of the non-nucleoside building blocks creates a foldamer structure that is stable in aqueous media.

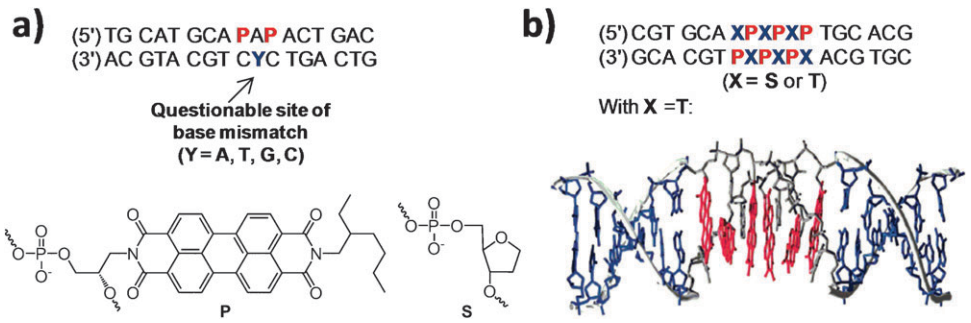

Fig. 16 The use of a PDI in combination with an acyclic linker for the detection of a single base mismatch (a) or to obtain a zipper-like recognition motif (b). (*Adapted with permission from ref. 128 Copyright 2008, Wiley-VCH.*)

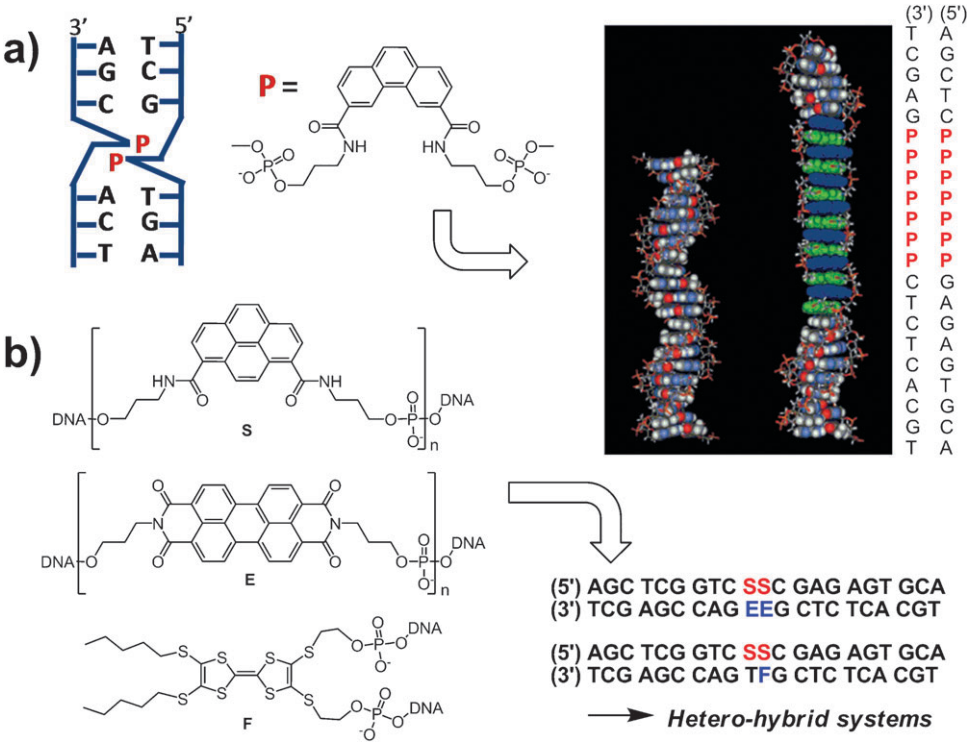

Fig. 17 (a) Phenanthrenyl linker used by Haner and schematic representation of the interstrand interaction between two of these linker molecules (left). Modelling of a 21-mer DNA duplex incorporating seven modified phenanthrene base pairs compared to the non-modified analogue (right) (*Adapted with permission from ref. 129 Copyright 2005, Wiley-VCH*). (b) Structures of Haner's pyrene, PDI and TTF linkers for the construction of heterohybrid DNA systems.

Following the same strategy, multiple pyrene residues were embedded inside a DNA duplex in an interstrand stacking arrangement (Fig. 17b).[130,131] A large stabilisation of the hybrid was observed if more than six artificial nucleosides were introduced ($\Delta T_m = +23$ °C in the case of seven modified base pairs). In addition to the interstrand stabilisation, intra-strand folding of the single chain was found to facilitate the duplex formation, likely by reducing the entropy change. Interestingly, CD spectroscopy measurements revealed that the pyrenes within the stack were arranged in a right-handed helical conformation, which was further confirmed by molecular modelling. The twisting of the stacked pyrenes was caused by the flanking nucleobases and driven by hydrophobic interactions and probably relayed by inter-strand H-bonding of the amide units. The helical organisation was found to have a profound influence on the fluorescence properties of the duplex. In the case of 14 stacked pyrenes, excimer-type fluorescence was observed in both duplex and single strand, and an unexpected blue shift in the excimer fluorescence was found to occur when the temperature was decreased. This behaviour is likely the result of the switching from a sandwich type arrangement of the stacked pyrenes to a twisting arrangement of these dye molecules. These studies were extended to hetero-hybrid systems. For instance, mixing pyrene and PDI type residues led to an alternating zipper like arrangement (SESE, see Fig. 17b) within the duplex allowing for a quenching of the fluorescence of the PDI units by the adjacent pyrenes.[132] When the pyrene residues were mixed with TTF units (Fig. 17b), a quenching of the pyrene fluorescence was observed. The latter process is likely to proceed through a photo-induced electron

transfer from the TTF to the pyrene residues in the stacked assembly.[133] Recently, also triazolylpyrenes[135] and alkynyl pyrenes,[134] have been included in these studies providing new scopes in the design of artificial double-stranded helices for applications in nanotechnology.

Second approach: outside stacking

The organisation of chromophores using DNA based skeletons while keeping the Watson–Crick interactions intact has been studied by the groups of Wagenknecht (DNA),[136–138] Stulz (DNA),[139–141] Yamana (RNA)[142–144] and Wengel (LNA).[145–150] Wagenknecht and co-workers applied the DNA base modification strategy to obtain helical stacks that consisted of up to five adjacent pyrenes. The chromophores were linked covalently to the uridine units by a C–C bond allowing for a strong electronic coupling (Fig. 18).[136] Melting temperature studies indicated that the incorporation of one pyrene unit destabilised the duplex but no additional destabilisation was observed in the case of five adjacent pyrenes. This showed that a certain amount of destabilisation was regained by the hydrophobic interaction between the chromophores. CD spectroscopy studies revealed an excitonic coupled CD signal in the wavelength range of the chromophore absorption band, which pointed to a right-handed helical arrangement of the pyrenes. The hybridisation of the modified DNA strand with its unmodified counter strand led to a strong enhancement in the fluorescence intensity, which was higher than the sum of the individual chromophores. In addition, a bathochromic shift of the emission maxima, which accounts for excitonic interactions in a regular and highly organised structure, was observed. The helical arrangement of the chromophores could tolerate the presence of one mismatch but was disrupted if two or more mismatches were present. A similar highly organised helical π-stacked arrangement of dyes along the major groove of duplex DNA was also obtained in the case of 1-ethynylpyrene, but only if more than three chromophores were synthetically incorporated adjacent to each other (deduced from CD measurements) (Fig. 18).[137] When five chromophores were present the fluorescence intensity turned out to be very sensitive to the incorporation of a single mismatch. By using two different chromophores (*i.e.* 5-(pyren-1-yl) and 5-(10-methylphenothiazin-3-yl), PyU and PzU, respectively),[138] it was possible to modulate the absorption and fluorescence properties of the assemblies, *i.e.* by varying the sequence of the chromophores within the π-arrays. These sequence specific assemblies of chromophores are potentially useful for the construction of optical nanodevices and as nucleic acid sensors for molecular diagnostics.

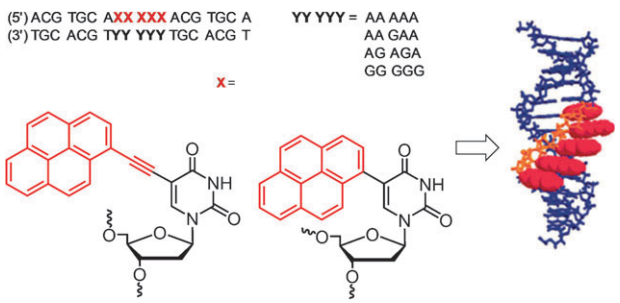

Fig. 18 Pyrene and 1-ethynylpyrene modified uridines used by Wagenknecht *et al.*

In their quest for porphyrin arrays, Stulz and co-workers introduced up to eleven porphyrins in a DNA chain through acetylene linkers attached to the 5 position of the 2′-deoxyuridines. Two architectures were investigated, one in which all the porphyrins were tethered to the same single strand, and one in which the porphyrins were placed on the two complementary strands in an alternating fashion, which led to very different features (Fig. 19). In the first case,[139] the porphyrins were aligned along the major groove of the duplex and displayed electronic interaction in the ground and excited states as a result of their helical stacking (see modelling in Fig. 19a). This was evidenced from a broadening of the porphyrin absorbance (Soret-band) and by the fact that the emission of the porphyrin arrays was quenched compared to the situation where the porphyrins were introduced non-adjacently. A strong destabilisation of the duplex by $\Delta T_m \sim 5$–7 °C per porphyrin modification was, however, observed as can be expected for such sterically demanding substituents. The situation was slightly improved when less bulky diphenylporphyrins were incorporated but destabilisation still occurred.[140]

Interestingly, the single strand itself adopted a helical elongated secondary structure, which was stable up to 55 °C in the case of eleven porphyrins. In this structure the porphyrins were also stacked as deduced from absorption and emission spectroscopy and from modelling studies (Fig. 19a). Compared to its duplex form, the porphyrin absorbance was lower and the emission was more quenched, which pointed to a more efficient stacking of the porphyrins in a more hydrophilic environment. This behaviour is in contrast to the pyrene-DNA/RNA arrays, where such a helical secondary structure stabilised by the stacking of the chromophores was never observed with a single strand. This has an obvious interest for the construction of photonic nano-wires.

In a second study,[141] Stulz and co-workers used another strategy and introduced the porphyrins onto the two complementary strands of a duplex, in such a way that a shift of one base in their positioning was present (Fig. 19b). This alternating arrangement led to a zipper-like assembly in which up to 11 porphyrins were aligned along the major groove and stacked by pairs involving one porphyrin of each strand in a zigzag fashion. In this case, no destabilisation of the duplex was found to occur if more than four porphyrins were introduced, which is likely due to the inter-strand interaction of the chromophores. Broadening of the porphyrin Soret-band and a decrease in the fluorescence intensity when lowering the temperature indicated that the porphyrins interacted electronically when stacked in the zipper array. Interestingly, this approach allowed the authors to insert a metal (Zn) in one of the two strands, which led to an alternate stacking of metal free and metal incorporated porphyrins in the duplex without loss of thermal stability (Fig. 19b). Energy transfer was effective in this system since, upon annealing of the free and metalated strands, fluorescence of the Zn-porphyrin was partially quenched whereas enhanced fluorescence of the free porphyrin was observed. These results highlight the potential

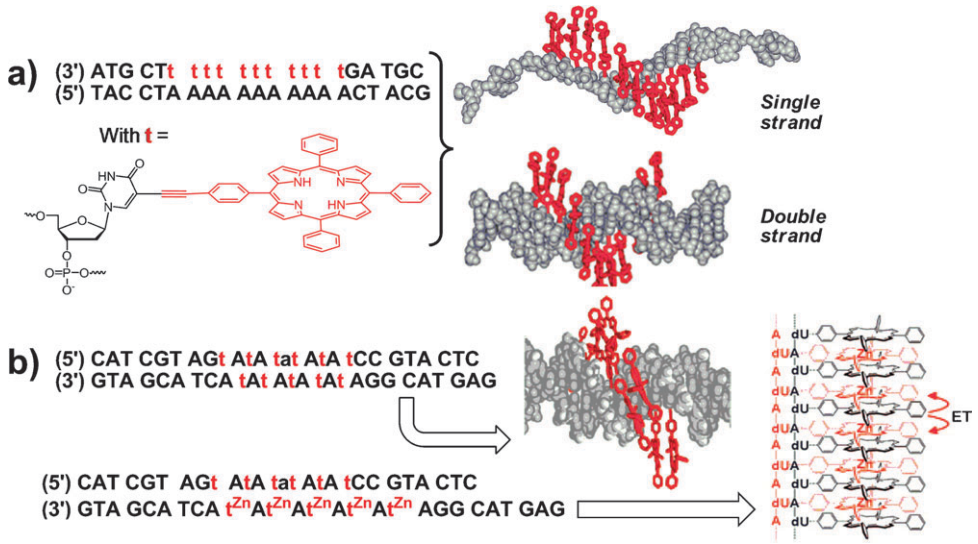

Fig. 19 (a) Structure of a porphyrin modified thymine nucleotide used for the construction of DNA helical arrays (*Adapted with permission from ref. 139 Copyright 2007, American Chemical Society*); (b) alternate stacking of metal-free and Zn-porphyrins in a DNA strand displaying energy transfer. (*Adapted with permission from ref. 141 Copyright 2009, Wiley-VCH.*)

of DNA as a scaffold to arrange metal ions on a nanometre scale, which obviously opens perspectives in the construction of nano-electronic and photonic wires.

Alternative strategies for the construction of DNA-based photonic wires: sequential chromophore arrays

In an alternative strategy, DNA molecules have been used as scaffolds to organise chromophores in the weakly coupled regime, the objective being the design of photonic wires. Donor and acceptor molecules are used to inject and release energy, and the transport of excited state energy is realised either by using a cascade of differently absorbing and emitting chromophores or by using similar chromophores as mediator units, which transport energy by hopping. Whereas the first strategy allows for unidirectional energy transport, it suffers from energy loss at each step of the process thereby limiting the length of the photonic wire. On the other hand, the latter strategy does not allow unidirectional energy transfer, which leads to a decrease in the overall end-to-end efficiency.

In early work, Shchepinov and co-workers designed a flexible system for multiple fluorescence resonance energy transfer (FRET) processes (see Fig. 20a).[151] The different chromophores (pyrene, perylene, fluorescein and tetramethylrhodamine) display overlapping absorption and emission spectra and sequential energy transfer across all four chromophores with high overall efficiency was observed. Interestingly, energy transfer was not detected when the propanediol linkers between each pair of fluorophores were absent, which suggested that a certain degree of freedom of the fluorophores was needed for the energy transfer to occur.

Improvement of this system can be realised by making use of a more rigid scaffold such as DNA. Sauer and co-workers investigated an energetic downhill cascade arrangement of five different chromophores that form an overlapping pathway for a unidirectional energy transfer (Fig. 20b).[152,153] For this purpose, the chromophores were attached to short oligonucleotides that were sequentially hybridised to a single strand DNA backbone. The chromophores are thus separated by a distance of 10 base pairs (*ca.* 3.4 nm), which does not allow the control of their relative orientation but prevents dimer formation, which is essential to avoid energy sinks (Fig. 20b). Ensemble fluorescence measurements revealed an end-to-end energy transfer efficiency of $\sim$0.15, which is much lower than the expected one based on theoretical considerations. To investigate the origin of the FRET efficiencies obtained in bulk measurements, single molecule fluorescence spectroscopy (SMFS) was used to probe, at the single molecular level, the sources of heterogeneity in the multistep energy transfer processes.[154,155] For this, the template DNA strand was grafted onto a glass surface. A subpopulation of $\sim$10% of the immobilized photonic wires showed a predominantly red emission, which corresponded to a unidirectional, highly efficient (up to 90%), multistep energy transfer over a distance of 13.6 nm and a spectral range of $\sim$200 nm. It was found that conformational freedom of the wire and partial DNA hybridisation led to multiple pathways for the photon emission. The use of DNA ligases to enhance the rigidity of the multi-chromophoric assemblies or the development of new labelling strategies to fix the conformation of the fluorophores might improve the efficiency of the energy transfer in these systems beyond five molecules.

Ohya and co-workers used the same strategy and introduced four chromophores with overlapping absorption and emission spectra, *i.e.* an eosine (Eo) molecule, one or two tetramethylrhodamine molecules and a Texas Red (TR) molecule as donor, mediator(s) and acceptor, respectively (Fig. 20c).[156] Multistep FRET from Eo to TR through the mediator(s) was observed over a distance of $\sim$10 nm with about 20% efficiency. Quake and co-workers followed a related strategy to construct nanometre-scale optical waveguides based on a repeating fluorophore for energy transport (Fig. 20d).[157]

Input (6-carboxyfluorescein, 6-FAM) and output (Cy5) molecules were tethered to the 3′ and 5′ end of a single DNA strand

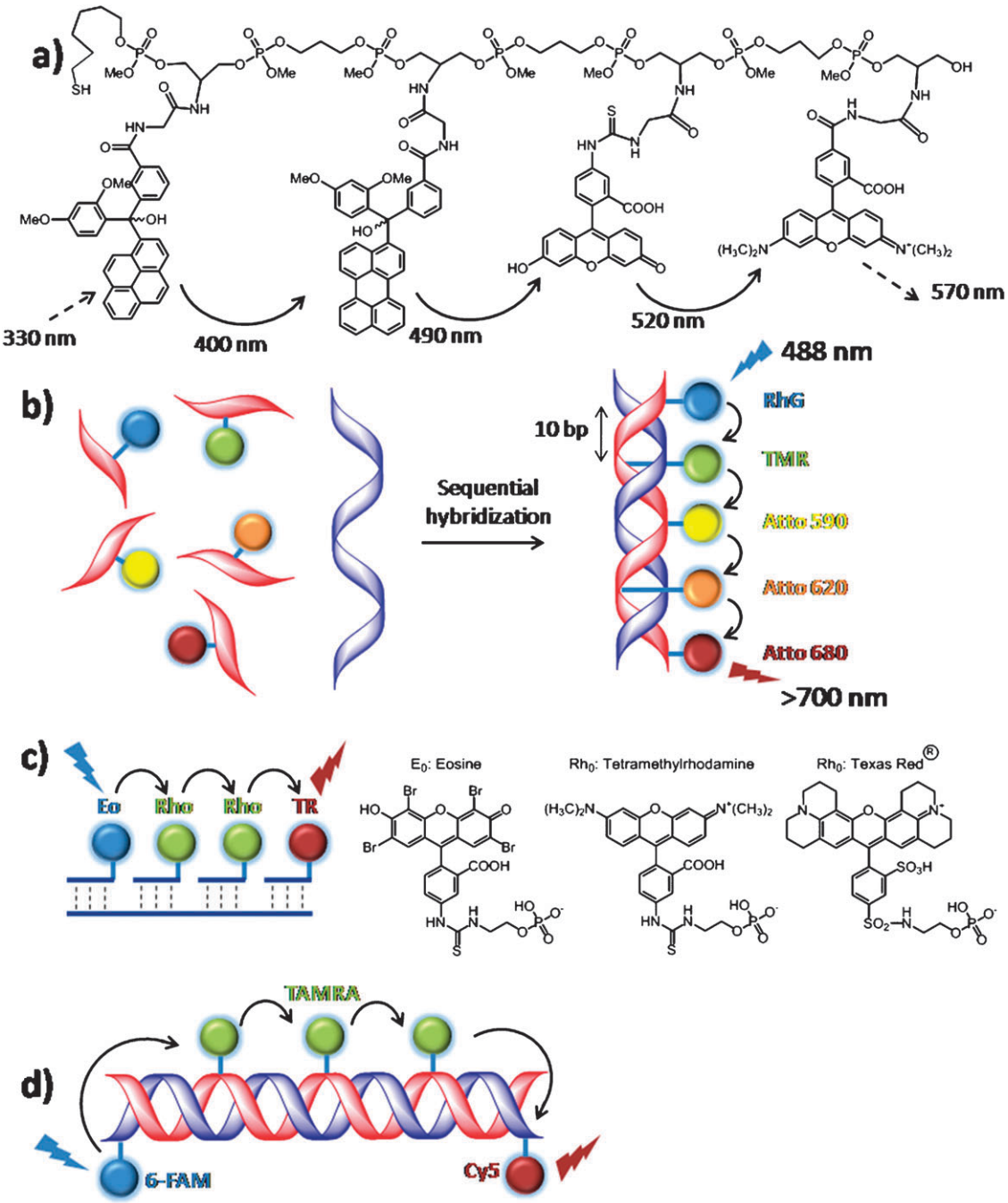

Fig. 20 (a) Sequential energy transfer across four chromophores tethered to a single-stranded acyclic backbone; (b) unidirectional multistep FRET with five chromophores arranged in an energetic down-hill cascade; (c) multistep FRET in sequential chromophore arrays assemblies; (d) quad-FRET assembly with 6-FAM, TAMRA and Cy5 as donor, repeating fluorophore and acceptor molecules, respectively.

that was hybridised with the complementary strand bearing three mediator molecules (6-tetramethylrhodamine-5(6)-carboxamide, TAMRA). The five chromophores are thereby separated from one other by 10 base pairs; quad-FRET efficiency of about 20% over the five chromophores was obtained.

The use of DNA as scaffold for the construction of chromophoric assemblies is still an emerging field, but one can already glimpse prospective applications, such as new fluorescent labelling agents, photonic nanowires, artificial base pairing, new recognition codes and charge transfer systems. It is clear that the programmability of DNA and its self-assembled architectures are ideal for the construction of precisely defined chromophoric nano objects with a high degree of modularity. Many exciting developments will without a doubt emerge from this approach.

5. Viruses

Viruses and virus-like particles (VLPs) have recently been receiving increased attention because of their tremendous

potential in the field of materials science.[158–160] These programmable and easily modifiable biological building blocks can serve as ideal scaffolds for nanomaterial based devices. In recent years VLPs have also been used as a scaffold to arrange chromophoric molecules in a well-defined spatial relationship. This approach is still in its early stages, but without a doubt very promising for the construction of unique biohybrid materials. A considerable advantage of the use of viruses is that their architectures are very precise and monodisperse as can be concluded from crystal structure studies. In addition, due to the advances in the biosciences, viruses can be readily modified leading to site specific positioning of the chromophores and hence exact control over the architecture of the final system up to sub nanometre resolution. In 2005, Francis and co-workers were the first to demonstrate that chromophoric molecules can be selectively attached to a virus.[161] By using standard peptide coupling conditions, a rhodamine derivative could be coupled to both the outer and inner surface of the tobacco mosaic virus (TMV).

Very high levels of modification, ~2100 external and ~650 internal sites per 300 nm rod, could be achieved without perturbing the stability of the assembled capsids. This elegant proof of principle paved the way for the construction of linear arrays of chromophores arranged in a well-defined fashion using the precise architecture of the TMV as a scaffold. In addition, the assembly properties of the TMV can be controlled and finely tuned by genetic modification of the TMV coat protein (TMVCP) monomers. By using recombinant TMVCP monomers bearing reactive cysteine groups on the loop of the monomer, a series of chromophores, for example, pyrenes,[162] porphyrins (see for example Fig. 21a)[163] and derivatised rhodamines,[164] could be introduced using 'maleimide chemistry'.

Depending on the pH of the system, zinc or free base porphyrin functionalised TMVCP building blocks could be assembled into double-layer disk-type assemblies or rod-type structures as analysed by AFM. To gain insight into the electronic properties of their system, different mixtures of the zinc (Zn) porphyrin TMVCP conjugates and free base (FB) porphyrin TMVCP conjugates were used to form a random mixture of chromophores in the TMV assembly (Fig. 21). The energy transfer rates (from Zn to FB) amounted to 3.1–6.4 × 10^9 s^{-1}, as determined by time-resolved fluorescence spectroscopy.[163]

Based on the same cysteine strategy, donors **24** and **25** and acceptor **26** were incorporated randomly into the TMV assembly (Fig. 22). The assemblies contained around ~700 chromophores per 100 nm rod with a spacing between the chromophores that is within the Förster radius for energy transfer between the dyes. The ability of the virus to precisely order the chromophores was illustrated by fluorescence measurements, which indicated that at least 20 donor chromophores can funnel energy into a single acceptor.[164] A more detailed understanding of the energy transfer processes in this system was obtained by time-resolved fluorescence spectroscopy (for a TMV conjugates with a **24** : **26** ratio of 100 : 1), which revealed that the energy transfer from **24** to **26** occurred in 187 ps with an efficiency of 36%. The three pathways for the dissipation of electronic energy from the excited state of the donor

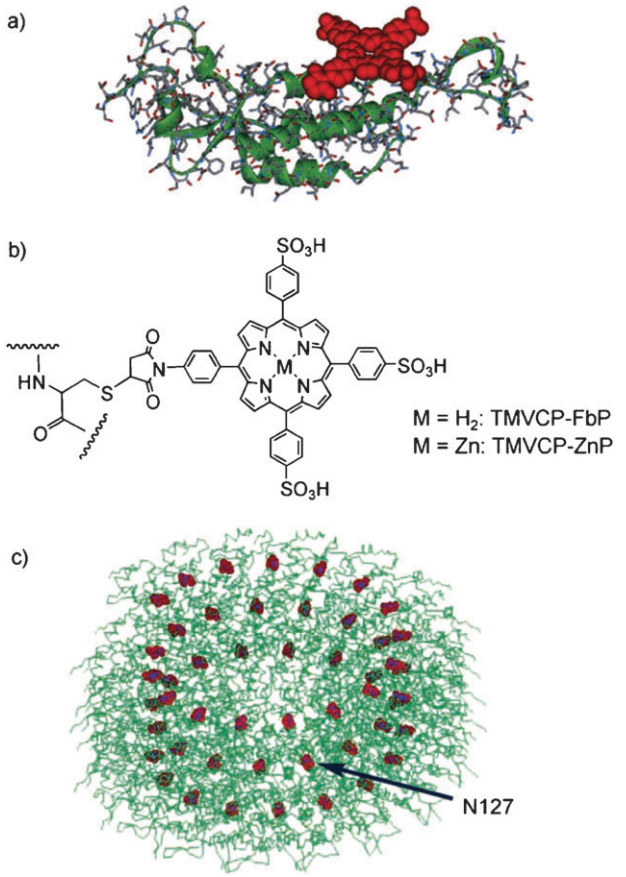

Fig. 21 (a) Structure of the TMVCP–porphyrin conjugated monomer; the porphyrin moiety was introduced at the amino acid position 127. (b) Chemical structure of the porphyrin used in the study of Majima and co-workers. Porphyrin derivatives were introduced to the cysteine residue of a TMV monomer through maleimido–thiol coupling. (c) Crystal structure of the TMV assembly with the amino acid N127 molecules shown in red. (*Adapted with permission from ref. 163 Copyright 2007, Wiley-VCH.*)

chromophore included donor emission, donor-to-donor transfer and donor-to-acceptor transfer.[165] The energy transfer values might be lower than those found in nature, yet as a first example they are comparable to other synthetic analogues, and the optimisation in the structural arrangement of the chromophores within the bioconjugates can be expected to lead to significant improvements in the future.

A non-covalent approach, in which cationic porphyrins were bound to the outer surface of a bacteriophage in a similar fashion to that reported for CNTs, was also recently reported.[166] Interestingly, a FRET from the external tryptophan residues of the phage to the interacting porphyrin molecules was clearly observed. A Förster radius of about 30 Å was calculated, which allows efficient transfer of excitation energy and is in agreement with a tryptophan residue being present in the N-terminal region of the phage. Bearing in mind that the ratio of tryptophan to porphyrin residues is roughly only 250 : 1, a careful design of the porphyrin–phage bioconjugate could further increase the efficiency as an antenna system. In this respect site directed mutagenesis and recombinant cloning techniques are efficient tools to realise this.

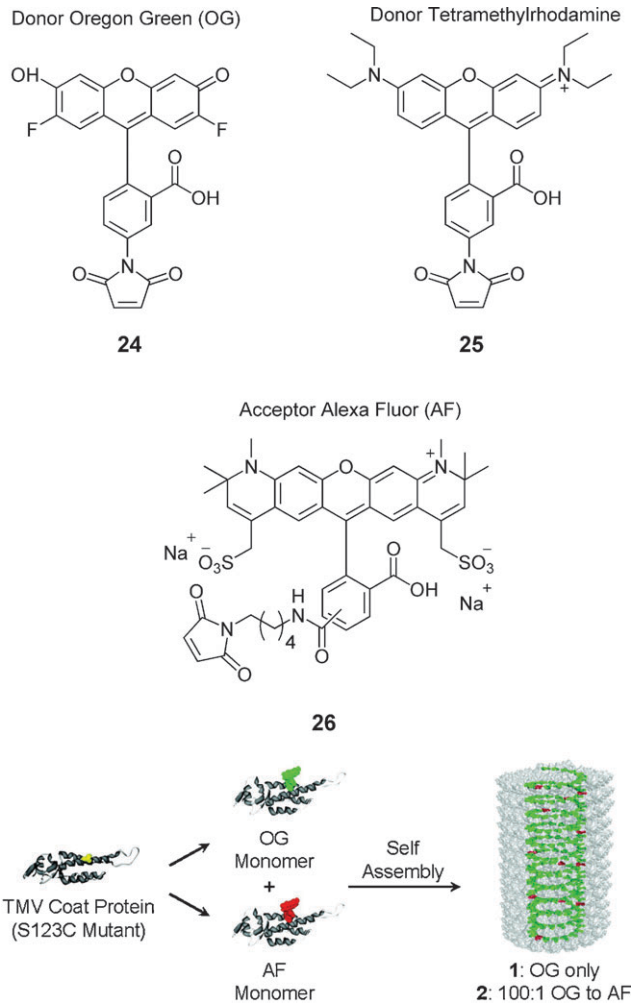

Fig. 22 Chemical structures of the donor (**24** and **25**) and acceptor (**26**) molecules used for the construction of chromophoric TMV conjugates. TMVP monomers labelled with either OG (**24**) or AF (**26**) were combined in a 100 : 1 ratio to form the rod-shaped assemblies. (*Adapted with permission from ref. 165 Copyright 2008, American Chemical Society.*)

6. Conclusion & outlook

In this review, four interesting macromolecular scaffolds to arrange extended π-conjugated chromophores, such as porphyrins, phthalocyanines, perylenes, pyrenes, into functional architectures have been described. They differ in structure, size, shape and physical properties and thus offer chemists and physicists a wide range of tools to play with. Inspired by the light harvesting systems in nature, various helical polymer scaffolds have been developed over the last years. Due to the versatility of the available synthetic procedures the polymers can be readily adjusted to meet the required specifications. The ordering of chromophores in space with the help of polymer scaffolds offers unique possibilities to prepare materials with new electronic and mechanical properties. For example, in the case of polyisocyanides, the helical nature of the polymer in combination with the fact that functional side-arms can be precisely positioned along the polymer backbone, results in unique molecules that can act as nanowires along which excitons can rapidly migrate. In the coming years, the incorporation of chromophores in a specific fashion, for example, to create a downhill energy path will be an interesting challenge.

The attachment of chromophores to CNTs has recently become a topic of increased research activity. Initially, the focus was more on the covalent attachment of the chromophores to the CNTs, but since this approach can lead to disruption of the π-system of the CNTs and hence in partial loss of electronic and structural properties, activities have been more directed towards non-covalent interactions. Elegant systems based on Coulombic, van der Waals, and/or π–π interactions have emerged in recent years. Comprehensive photophysical studies of the chromophore–CNT hybrids have given more insights in the physical processes that take place offering interesting possibilities for materials with new and promising electronic properties. The synthetic work together with the detailed spectroscopic characterisations have paved the way for applying these hybrids in organic electronic devices in the coming years.

Natural systems are currently receiving great interest as scaffolds for chromophoric molecules. It is evident that DNA, with its programmable architecture, offers unique possibilities for this purpose, but this field is still in its early stages and many scouting studies are still needed. Like DNA, viruses also offer a programmable and easily modifiable building block for the creation of nanomaterials. Although in its early stages, significant progress has already been made by various groups and it can be expected that further optimisation of the virus–chromophore constructs will lead to significant improvements and hence interesting applications in the near future.

Acknowledgements

The Technology Foundation STW, NanoNed, The Council for the Chemical Sciences of the Netherlands Organisation for Scientific Research, and the Royal Academy for Arts and Sciences are acknowledged for financial support.

References

1 J. M. Lehn, *Science*, 2002, **295**, 2400–2403.
2 G. M. Whitesides, J. P. Mathias and C. T. Seto, *Science*, 1991, **254**, 1312–1319.
3 M. Kasha, *Spectrochim. Acta*, 1958, **12**, 386–386.
4 E. G. Mcrae and M. Kasha, *J. Chem. Phys.*, 1958, **28**, 721–722.
5 G. Mcdermott, S. M. Prince, A. A. Freer, A. M. Hawthornthwaitelawless, M. Z. Papiz, R. J. Cogdell and N. W. Isaacs, *Nature*, 1995, **374**, 517–521.
6 R. v. Grondelle, J. P. Dekker, T. Gillbro and V. Sundstrom, *Biochim. Biophys. Acta, Bioenerg.*, 1994, **1187**, 1–65.
7 S. Bahatyrova, R. N. Frese, K. O. van der Werf, C. Otto, C. N. Hunter and J. D. Olsen, *J. Biol. Chem.*, 2004, **279**, 21327–21333.
8 G. R. Fleming and R. vanGrondelle, *Curr. Opin. Struct. Biol.*, 1997, **7**, 738–748.
9 J. Linnanto and J. E. I. Korppi-Tommola, *Phys. Chem. Chem. Phys.*, 2002, **4**, 3453–3460.
10 T. Pullerits and V. Sundstrom, *Acc. Chem. Res.*, 1996, **29**, 381–389.
11 S. Scheuring, J. Seguin, S. Marco, D. Levy, B. Robert and J. L. Rigaud, *Proc. Natl. Acad. Sci. U. S. A.*, 2003, **100**, 1690–1693.

12 A. W. Bosman, H. M. Janssen and E. W. Meijer, *Chem. Rev.*, 1999, **99**, 1665–1688.
13 F. C. De Schryver, T. Vosch, M. Cotlet, M. Van der Auweraer, K. Mullen and J. Hofkens, *Acc. Chem. Res.*, 2005, **38**, 514–522.
14 A. P. H. J. Schenning and E. W. Meijer, *Chem. Commun.*, 2005, 3245–3258.
15 F. J. M. Hoeben, P. Jonkheijm, E. W. Meijer and A. Schenning, *Chem. Rev.*, 2005, **105**, 1491–1546.
16 X. Schultze, J. Serin, A. Adronov and J. M. J. Frechet, *Chem. Commun.*, 2001, 1160–1161.
17 F. X. Redl, M. Lutz and J. Daub, *Chem.–Eur. J.*, 2001, **7**, 5350–5358.
18 J. Cornelissen, A. E. Rowan, R. J. M. Nolte and N. Sommerdijk, *Chem. Rev.*, 2001, **101**, 4039–4070.
19 T. Nakano and Y. Okamoto, *Chem. Rev.*, 2001, **101**, 4013–4038.
20 G. Natta, P. Pino, P. Corradini, F. Danusso, E. Mantica, G. Mazzanti and G. Moraglio, *J. Am. Chem. Soc.*, 1955, **77**, 1708–1710.
21 J. W. Y. Lam and B. Z. Tang, *Acc. Chem. Res.*, 2005, **38**, 745–754.
22 E. Yashima and K. Maeda, in *Foldamers: Structure, Properties, and Applications*, ed. S. Hecht and I. Huc, Wiley-VCH, Weinheim, 2007, pp. 331–366.
23 E. Yashima, K. Maeda and Y. Furusho, *Acc. Chem. Res.*, 2008, **41**, 1166–1180.
24 M. M. Green, N. C. Peterson, T. Sato, A. Teramoto, R. Cook and S. Lifson, *Science*, 1995, **268**, 1860–1866.
25 G. Koeckelberghs, M. Van Beylen and C. Samyn, *Mater. Sci. Eng.,C*, 2001, **18**, 15–20.
26 S. Mayer, G. Maxein and R. Zentel, *Macromolecules*, 1998, **31**, 8522–8525.
27 S. Mayer and R. Zentel, *Macromol. Chem. Phys.*, 1998, **199**, 1675–1682.
28 M. M. Green, B. A. Garetz, B. Munoz, H. P. Chang, S. Hoke and R. G. Cooks, *J. Am. Chem. Soc.*, 1995, **117**, 4181–4182.
29 M. Fujiki, *Macromol. Rapid Commun.*, 2001, **22**, 539–563.
30 H. D. Tang, Y. Y. Liu, B. Huang, J. G. Qin, C. Fuentes-Hernandez, B. Kippelen, S. J. Li and C. Ye, *J. Mater. Chem.*, 2005, **15**, 778–784.
31 A. Goodwin and B. M. Novak, *Macromolecules*, 1994, **27**, 5520–5522.
32 H. Z. Tang, E. R. Garland, B. M. Novak, J. T. He, P. L. Polavarapu, F. C. Sun and S. S. Sheiko, *Macromolecules*, 2007, **40**, 3575–3580.
33 H. Z. Tang, B. M. Novak, J. T. He and P. L. Polavarapu, *Angew. Chem., Int. Ed.*, 2005, **44**, 7298–7301.
34 H. Z. Tang, P. D. Boyle and B. M. Novak, *J. Am. Chem. Soc.*, 2005, **127**, 2136–2142.
35 G. L. Tian, Y. J. Lu and B. M. Novak, *J. Am. Chem. Soc.*, 2004, **126**, 4082–4083.
36 H. Z. Tang, Y. J. Lu, G. L. Tian, M. D. Capracotta and B. M. Novak, *J. Am. Chem. Soc.*, 2004, **126**, 3722–3723.
37 Y. Okamoto and T. Nakano, *Chem. Rev.*, 1994, **94**, 349–372.
38 R. J. M. Nolte, A. J. M. Van Beijnen and W. Drenth, *J. Am. Chem. Soc.*, 1974, **96**, 5932–5933.
39 R. J. M. Nolte, *Chem. Soc. Rev.*, 1994, **23**, 11–19.
40 M. Suginome and Y. Ito, *Adv. Polym. Sci.*, 2004, **171**, 77–136.
41 B. Hong and M. A. Fox, *Macromolecules*, 1994, **27**, 5311–5317.
42 B. Hong and M. A. Fox, *Can. J. Chem.*, 1995, **73**, 2101–2110.
43 M. N. Teerenstra, J. G. Hagting, A. J. Schouten, R. J. M. Nolte, M. Kauranen, T. Verbiest and A. Persoons, *Macromolecules*, 1996, **29**, 4876–4879.
44 M. Kauranen, T. Verbiest, E. W. Meijer, E. E. Havinga, M. N. Teerenstra, A. J. Schouten, R. J. M. Nolte and A. Persoons, *Adv. Mater.*, 1995, **7**, 641–644.
45 M. Kauranen, T. Verbiest, C. Boutton, M. N. Teerenstra, K. Clays, A. J. Schouten, R. J. M. Nolte and A. Persoons, *Science*, 1995, **270**, 966–969.
46 M. N. Teerenstra, R. D. Klap, M. J. Bijl, A. J. Schouten, R. J. M. Nolte, T. Verbiest and A. Persoons, *Macromolecules*, 1996, **29**, 4871–4875.
47 E. Gomar-Nadal, L. Mugica, J. Vidal-Gancedo, J. Casado, J. T. L. Navarrete, J. Veciana, C. Rovira and D. B. Amabilino, *Macromolecules*, 2007, **40**, 7521–7531.
48 E. Gomar-Nadal, J. Veciana, C. Rovira and D. B. Amabilino, *Adv. Mater.*, 2005, **17**, 2095–2098.
49 N. Hida, F. Takei, K. Onitsuka, K. Shiga, S. Asaoka, T. Iyoda and S. Takahashi, *Angew. Chem., Int. Ed.*, 2003, **42**, 4349–4352.
50 K. Onitsuka, T. Joh and S. Takahashi, *Angew. Chem., Int. Ed.*, 1992, **104**, 851–852.
51 J. A. A. W. Elemans, R. Van Hameren, R. J. M. Nolte and A. E. Rowan, *Adv. Mater.*, 2006, **18**, 1251–1266.
52 J. H. Chou, M. E. Kosal, H. S. Nalwa, N. A. Rakow and K. S. Suslick, *The Porphyrin Handbook*, Academic Press, New York, 2000, vol. 6.
53 F. Takei, K. Onitsuka, N. Kobayashi and S. Takahashi, *Chem. Lett.*, 2000, 914–915.
54 F. Takei, H. Hayashi, K. Onitsuka, N. Kobayashi and S. Takahashi, *Angew. Chem., Int. Ed.*, 2001, **40**, 4092–4094.
55 F. Takei, S. Nakamura, K. Onitsuka, A. Ishida, S. Tojo, T. Majima and S. Takahashi, *Chem. Lett.*, 2003, **32**, 506–507.
56 F. Takei, D. Kodama, S. Nakamura, K. Onitsuka and S. Takahashi, *J. Polym. Sci., Part A: Polym. Chem.*, 2006, **44**, 585–595.
57 M. Fujitsuka, A. Okada, S. Tojo, F. Takei, K. Onitsuka, S. Takahashi and T. Majima, *J. Phys. Chem. B*, 2004, **108**, 11935–11941.
58 J. A. S. J. Razenberg, A. W. Vandermade, J. W. H. Smeets and R. J. M. Nolte, *J. Mol. Catal.*, 1985, **31**, 271–287.
59 P. A. J. de Witte, M. Castriciano, J. J. L. M. Cornelissen, L. M. Scolaro, R. J. M. Nolte and A. E. Rowan, *Chem.–Eur. J.*, 2003, **9**, 1775–1781.
60 S. Matile, N. Berova, K. Nakanishi, S. Novkova, I. Philipova and B. Blagoev, *J. Am. Chem. Soc.*, 1995, **117**, 7021–7022.
61 S. Matile, N. Berova, K. Nakanishi, J. Fleischhauer and R. W. Woody, *J. Am. Chem. Soc.*, 1996, **118**, 5198–5206.
62 N. Berova, K. Nakanishi and R. W. Woody, *Circular Dichroism: Principles and Applications*, Wiley-VCH, New York, 2nd edn, 2000.
63 J. J. L. M. Cornelissen, J. J. J. M. Donners, R. de Gelder, W. S. Graswinckel, G. A. Metselaar, A. E. Rowan, N. A. Sommerdijk and R. J. M. Nolte, *Science*, 2001, **293**, 676–680.
64 P. Samori, C. Ecker, I. Goessl, P. A. J. de Witte, J. J. L. M. Cornelissen, G. A. Metselaar, M. B. J. Otten, A. E. Rowan, R. J. M. Nolte and J. P. Rabe, *Macromolecules*, 2002, **35**, 5290–5294.
65 P. A. J. de Witte, J. Hernando, E. E. Neuteboom, E. M. H. P. van Dijk, S. C. J. Meskers, R. A. J. Janssen, N. F. van Hulst, R. J. M. Nolte, M. F. Garcia-Parajo and A. E. Rowan, *J. Phys. Chem. B*, 2006, **110**, 7803–7812.
66 J. Hernando, P. A. J. de Witte, E. M. H. P. van Dijk, J. Korterik, R. J. M. Nolte, A. E. Rowan, M. F. Garcia-Parajo and N. F. van Hulst, *Angew. Chem., Int. Ed.*, 2004, **43**, 4045–4049.
67 V. Palermo, M. B. J. Otten, A. Liscio, E. Schwartz, P. A. J. de Witte, M. A. Castriciano, M. M. Wienk, F. Nolde, G. De Luca, J. J. L. M. Cornelissen, R. A. J. Janssen, K. Mullen, A. E. Rowan, R. J. M. Nolte and P. Samori, *J. Am. Chem. Soc.*, 2008, **130**, 14605–14614.
68 C. E. Finlayson, R. H. Friend, M. B. J. Otten, E. Schwartz, J. Cornelissen, R. L. M. Nolte, A. E. Rowan, P. Samori, V. Palermo, A. Liscio, K. Peneva, K. Mullen, S. Trapani and D. Beljonne, *Adv. Funct. Mater.*, 2008, **18**, 3947–3955.
69 S. Foster, C. E. Finlayson, P. E. Keivanidis, Y.-S. Huang, I. Hwang, R. H. Friend, M. B. J. Otten, L. P. Lu, E. Schwartz, R. J. M. Nolte and A. E. Rowan, *Macromolecules*, 2009, **42**, 2023–2030.
70 E. Schwartz, V. Palermo, C. E. Finlayson, Y.-S. Huang, M. B. J. Otten, A. Liscio, S. Trapani, I. González-Valls, P. Brocorens, J. J. L. M. Cornelissen, K. Peneva, K. Müllen, F. Spano, A. Yartsev, S. Westenhoff, R. H. Friend, D. Beljonne, R. J. M. Nolte, P. Samori and A. E. Rowan, *Chem.–Eur. J.*, 2009, **15**, 2536–2547.
71 H. J. Kitto, E. Schwartz, M. Nijemeisland, M. Koepf, J. Cornelissen, A. E. Rowan and R. J. M. Nolte, *J. Mater. Chem.*, 2008, **18**, 5615–5624.
72 E. Schwartz, H. J. Kitto, R. de Gelder, R. J. M. Nolte, A. E. Rowan and J. J. L. M. Cornelissen, *J. Mater. Chem.*, 2007, **17**, 1876–1884.
73 C. R. Martin and P. Kohli, *Nat. Rev. Drug Discovery*, 2003, **2**, 29–37.

74 A. Bianco, K. Kostarelos and M. Prato, *Curr. Opin. Chem. Biol.*, 2005, **9**, 674–679.
75 M. Prato, K. Kostarelos and A. Bianco, *Acc. Chem. Res.*, 2008, **41**, 60–68.
76 L. Lacerda, A. Bianco, M. Prato and K. Kostarelos, *Adv. Drug Delivery Rev.*, 2006, **58**, 1460–1470.
77 H. P. Li, R. B. Martin, B. A. Harruff, R. A. Carino, L. F. Allard and Y. P. Sun, *Adv. Mater.*, 2004, **16**, 896–900.
78 D. Baskaran, J. W. Mays, X. P. Zhang and M. S. Bratcher, *J. Am. Chem. Soc.*, 2005, **127**, 6916–6917.
79 B. Ballesteros, S. Campidelli, G. de la Torre, C. Ehli, D. M. Guldi, M. Prato and T. Torres, *Chem. Commun.*, 2007, 2950–2952.
80 S. Campidelli, B. Ballesteros, A. Filoramo, D. D. Diaz, G. de la Torre, T. Torres, G. M. A. Rahman, C. Ehli, D. Kiessling, F. Werner, V. Sgobba, D. M. Guldi, C. Cioffi, M. Prato and J. P. Bourgoin, *J. Am. Chem. Soc.*, 2008, **130**, 11503–11509.
81 M. A. Herranz, N. Martin, S. P. Campidelli, M. Prato, G. Brehm and D. M. Guldi, *Angew. Chem., Int. Ed.*, 2006, **45**, 4478–4482.
82 Y. Xu, Z. Liu, X. Zhang, Y. Wang, J. Tian, Y. Huang, Y. Ma, X. Zhang and Y. Chen, *Adv. Mater.*, 2009, **21**, 1–5.
83 H. Murakami, T. Nomura and N. Nakashima, *Chem. Phys. Lett.*, 2003, **378**, 481–485.
84 H. P. Li, B. Zhou, Y. Lin, L. R. Gu, W. Wang, K. A. S. Fernando, S. Kumar, L. F. Allard and Y. P. Sun, *J. Am. Chem. Soc.*, 2004, **126**, 1014–1015.
85 F. Y. Cheng and A. Adronov, *Chem.–Eur. J.*, 2006, **12**, 5053–5059.
86 A. Satake, Y. Miyajima and Y. Kobuke, *Chem. Mater.*, 2005, **17**, 716–724.
87 D. M. Guldi, H. Taieb, G. M. A. Rahman, N. Tagmatarchis and M. Prato, *Adv. Mater.*, 2005, **17**, 871–875.
88 T. Hasobe, S. Fukuzumi and P. V. Kamat, *J. Am. Chem. Soc.*, 2005, **127**, 11884–11885.
89 D. M. Guldi, G. M. A. Rahman, M. Prato, N. Jux, S. H. Qin and W. Ford, *Angew. Chem., Int. Ed.*, 2005, **44**, 2015–2018.
90 G. M. A. Rahman, A. Troeger, V. Sgobba, D. M. Guldi, N. Jux, M. N. Tchoul, W. T. Ford, A. Mateo-Alonso and M. Prato, *Chem.–Eur. J.*, 2008, **14**, 8837–8846.
91 X. B. Wang, Y. Q. Liu, W. F. Qiu and D. B. Zhu, *J. Mater. Chem.*, 2002, **12**, 1636–1639.
92 G. M. A. Rahman, D. M. Guldi, S. Campidelli and M. Prato, *J. Mater. Chem.*, 2006, **16**, 62–65.
93 J. Y. Chen and C. P. Collier, *J. Phys. Chem. B*, 2005, **109**, 7605–7609.
94 D. M. Guldi, G. M. A. Rahman, N. Jux, N. Tagmatarchis and M. Prato, *Angew. Chem., Int. Ed.*, 2004, **43**, 5526–5530.
95 C. Ehli, G. M. A. Rahman, N. Jux, D. Balbinot, D. M. Guldi, F. Paolucci, M. Marcaccio, D. Paolucci, M. Melle-Franco, F. Zerbetto, S. Campidelli and M. Prato, *J. Am. Chem. Soc.*, 2006, **128**, 11222–11231.
96 C. Ehli, D. M. Guldi, M. A. Herranz, N. Martin, S. Campidelli and M. Prato, *J. Mater. Chem.*, 2008, **18**, 1498–1503.
97 M. A. Herranz, C. Ehli, S. Campidelli, M. Gutierrez, G. L. Hug, K. Ohkubo, S. Fukuzumi, M. Prato, N. Martin and D. M. Guldi, *J. Am. Chem. Soc.*, 2008, **130**, 66–73.
98 M. Inagaki, K. Kaneko and T. Nishizawa, *Carbon*, 2004, **42**, 1401–1417.
99 G. Pagona, A. S. D. Sandanayaka, A. Maigne, J. Fan, G. C. Papavassiliou, L. D. Petsalakis, B. R. Steele, M. Yudasaka, S. Iijima, N. Tagmatarchis and O. Ito, *Chem.–Eur. J.*, 2007, **13**, 7600–7607.
100 G. Pagona, A. S. D. Sandanayaka, Y. Araki, J. Fan, N. Tagmatarchis, M. Yudasaka, S. Iijima and O. Ito, *J. Phys. Chem. B*, 2006, **110**, 20729–20732.
101 G. Pagona, A. S. D. Sandanayaka, T. Hasobe, G. Charalambidis, A. G. Coutsolelos, M. Yudasaka, S. Iijima and N. Tagmatarchis, *J. Phys. Chem. C*, 2008, **112**, 15735–15741.
102 G. Pagona, A. S. D. Sandanayaka, Y. Araki, J. Fan, N. Tagmatarchis, G. Charalambidis, A. G. Coutsolelos, B. Boitrel, M. Yudasaka, S. Iijima and O. Ito, *Adv. Funct. Mater.*, 2007, **17**, 1705–1711.
103 C. Cioffi, S. Campidelli, C. Sooambar, M. Marcaccio, G. Marcolongo, M. Meneghetti, D. Paolucci, F. Paolucci, C. Ehli, G. M. A. Rahman, V. Sgobba, D. M. Guldi and M. Prato, *J. Am. Chem. Soc.*, 2007, **129**, 3938–3945.
104 M. Zhang, T. Murakami, K. Ajima, K. Tsuchida, A. S. D. Sandanayaka, O. Ito, S. Iijima and M. Yudasaka, *Proc. Natl. Acad. Sci. U. S. A.*, 2008, **105**, 14773–14778.
105 D. M. Guldi, G. M. A. Rahman, F. Zerbetto and M. Prato, *Acc. Chem. Res.*, 2005, **38**, 871–878.
106 N. C. Seeman, *Nature*, 2003, **421**, 427–431.
107 H.-A. Wagenknecht, *Angew. Chem., Int. Ed.*, 2009, **48**, 2838–2841.
108 R. Varghese and H.-A. Wagenknecht, *Chem. Commun.*, 2009, 2615–2624.
109 J. Gao, C. Strassler, D. Tahmassebi and E. T. Kool, *J. Am. Chem. Soc.*, 2002, **124**, 11590–11591.
110 J. N. Wilson, J. M. Gao and E. T. Kool, *Tetrahedron*, 2007, **63**, 3427–3433.
111 J. N. Wilson, Y. Cho, S. Tan, A. Cuppoletti and E. T. Kool, *ChemBioChem*, 2008, **9**, 279–285.
112 A. Cuppoletti, Y. Cho, J.-S. Park, C. Strassler and E. T. Kool, *Bioconjugate Chem.*, 2005, **16**, 528–534.
113 J. Gao, S. Watanabe and E. T. Kool, *J. Am. Chem. Soc.*, 2004, **126**, 12748–12749.
114 Y. N. Teo, J. N. Wilson and E. T. Kool, *J. Am. Chem. Soc.*, 2009, **131**, 3923–3933.
115 J. Chiba, S. Takeshima, K. Mishima, H. Maeda, Y. Nanai, K. Mizuno and M. Inouye, *Chem.–Eur. J.*, 2007, **13**, 8124–8130.
116 C. Brotschi, A. Häberli and C. J. Leumann, *Angew. Chem., Int. Ed.*, 2001, **40**, 3012–3014.
117 C. Brotschi and C. J. Leumann, *Angew. Chem., Int. Ed.*, 2003, **42**, 1655–1658.
118 N. A. Grigorenko and C. J. Leumann, *Chem. Commun.*, 2008, 5417–5419.
119 N. A. Grigorenko and C. J. Leumann, *Chem.–Eur. J.*, 2009, **15**, 639–645.
120 H. Asanuma, K. Shirasuka, T. Takarada, H. Kashida and M. Komiyama, *J. Am. Chem. Soc.*, 2003, **125**, 2217–2223.
121 H. Kashida, H. Asanuma and M. Komiyama, *Angew. Chem., Int. Ed.*, 2004, **43**, 6522–6525.
122 H. Kashida, M. Tanaka, S. Baba, T. Sakamoto, G. Kawai, H. Asanuma and M. Komiyama, *Chem.–Eur. J.*, 2006, **12**, 777–784.
123 H. Kashida, T. Fujii and H. Asanuma, *Org. Biomol. Chem.*, 2008, **6**, 2892–2899.
124 H. Asanuma, X. Liang, H. Nishioka, D. Matsunaga, M. Liu and M. Komiyama, *Nat. Protoc.*, 2007, **2**, 203–212.
125 X. G. Liang, H. Nishioka, N. Takenaka and H. Asanuma, *ChemBioChem*, 2008, **9**, 702–705.
126 C. Wagner and H.-A. Wagenknecht, *Org. Lett.*, 2006, **8**, 4191–4194.
127 D. Baumstark and H.-A. Wagenknecht, *Angew. Chem., Int. Ed.*, 2008, **47**, 2612–2614.
128 D. Baumstark and H. A. Wagenknecht, *Chem.–Eur. J.*, 2008, **14**, 6640–6645.
129 S. M. Langenegger and R. Haner, *ChemBioChem*, 2005, **6**, 2149–2152.
130 V. L. Malinovskii, F. Samain and R. Haner, *Angew. Chem., Int. Ed.*, 2007, **46**, 4464–4467.
131 D. Lindegaard, A. S. Madsen, I. V. Astakhova, A. D. Malakhov, B. R. Babu, V. A. Korshun and J. Wengel, *Bioorg. Med. Chem.*, 2008, **16**, 94–99.
132 N. Bouquin, V. L. Malinovskii and R. Haner, *Chem. Commun.*, 2008, 1974–1976.
133 N. Bouquin, V. L. Malinovskii, X. Guegano, S. X. Liu, S. Decurtins and R. Haner, *Chem.–Eur. J.*, 2008, **14**, 5732–5736.
134 H. Bittermann, D. Siegemund, V. L. Malinovskii and R. Haner, *J. Am. Chem. Soc.*, 2008, **130**, 15285–15287.
135 S. Werder, V. L. Malinovskii and R. Haner, *Org. Lett.*, 2008, **10**, 2011–2014.
136 E. Mayer-Enthart and H. A. Wagenknecht, *Angew. Chem., Int. Ed.*, 2006, **45**, 3372–3375.
137 J. Barbaric and H. A. Wagenknecht, *Org. Biomol. Chem.*, 2006, **4**, 2088–2090.
138 E. Mayer-Enthart, C. Wagner, J. Barbaric and H. A. Wagenknecht, *Tetrahedron*, 2007, **63**, 3434–3439.

139 L. A. Fendt, I. Bouamaied, S. Thoni, N. Amiot and E. Stulz, *J. Am. Chem. Soc.*, 2007, **129**, 15319–15329.
140 I. Bouamaied, T. Nguyen, T. Ruhl and E. Stulz, *Org. Biomol. Chem.*, 2008, **6**, 3888–3891.
141 T. Nguyen, A. Brewer and E. Stulz, *Angew. Chem., Int. Ed.*, 2009, **48**, 1974–1977.
142 M. Nakamura, Y. Ohtoshi and K. Yamana, *Chem. Commun.*, 2005, 5163–5165.
143 M. Nakamura, Y. Shimomura, Y. Ohtoshi, K. Sasa, H. Hayashi, H. Nakano and K. Yamana, *Org. Biomol. Chem.*, 2007, **5**, 1945–1951.
144 M. Nakamura, Y. Murakami, K. Sasa, H. Hayashi and K. Yamana, *J. Am. Chem. Soc.*, 2008, **130**, 6904–6905.
145 M. D. Sorensen, M. Petersen and J. Wengel, *Chem. Commun.*, 2003, 2130–2131.
146 P. J. Hrdlicka, B. R. Babu, M. D. Sorensen and J. Wengel, *Chem. Commun.*, 2004, 1478–1479.
147 P. J. Hrdlicka, B. R. Babu, M. D. Sorensen, N. Harrit and J. Wengel, *J. Am. Chem. Soc.*, 2005, **127**, 13293–13299.
148 T. S. Kumar, A. S. Madsen, M. E. Ostergaard, J. Wengel and P. J. Hrdlicka, *J. Org. Chem.*, 2008, **73**, 7060–7066.
149 I. V. Astakhova, V. A. Korshun, K. Jahn, J. Kjems and J. Wengel, *Bioconjugate Chem.*, 2008, **19**, 1995–2007.
150 I. V. Astakhova, V. A. Korshun and J. Wengel, *Chem.–Eur. J.*, 2008, **14**, 11010–11026.
151 M. S. Shchepinov and V. A. Korshun, *Nucleosides, Nucleotides Nucleic Acids*, 2001, **20**, 369–374.
152 M. Heilemann, P. Tinnefeld, G. S. Mosteiro, M. G. Parajo, N. F. Van Hulst and M. Sauer, *J. Am. Chem. Soc.*, 2004, **126**, 6514–6515.
153 P. Tinnefeld, M. Heilemann and M. Sauer, *ChemPhysChem*, 2005, **6**, 217–222.
154 M. Heilemann, R. Kasper, P. Tinnefeld and M. Sauer, *J. Am. Chem. Soc.*, 2006, **128**, 16864–16875.
155 G. Sanchez-Mosteiro, E. M. H. P. van Dijk, J. Hernando, M. Heilemann, P. Tinnefeld, M. Sauer, F. Koberlin, M. Patting, M. Wahl, R. Erdmann, N. F. van Hulst and M. F. Garcia-Parajo, *J. Phys. Chem. B*, 2006, **110**, 26349–26353.
156 Y. Ohya, K. Yabuki, M. Hashimoto, A. Nakajima and T. Ouchi, *Bioconjugate Chem.*, 2003, **14**, 1057–1066.
157 S. Vyawahare, S. Eyal, K. D. Mathews and S. R. Quake, *Nano Lett.*, 2004, **4**, 1035–1039.
158 M. Manchester and N. F. Steinmetz, *Current Topics in Microbiology and Immunology, Viruses and Nanotechnology*, Springer, Heidelberg, 2009, vol. 327.
159 M. Young, D. Willits, M. Uchida and T. Douglas, *Annu. Rev. Phytopathol.*, 2008, **46**, 361–384.
160 M. Comellas-Aragones, H. Engelkamp, V. I. Claessen, N. A. J. M. Sommerdijk, A. E. Rowan, P. C. M. Christianen, J. C. Maan, B. J. M. Verduin, J. J. L. M. Cornelissen and R. J. M. Nolte, *Nat. Nanotechnol.*, 2007, **2**, 635–639.
161 T. L. Schlick, Z. B. Ding, E. W. Kovacs and M. B. Francis, *J. Am. Chem. Soc.*, 2005, **127**, 3718–3723.
162 M. Endo, H. X. Wang, M. Fujitsuka and T. Majima, *Chem.–Eur. J.*, 2006, **12**, 3735–3740.
163 M. Endo, M. Fujitsuka and T. Majima, *Chem.–Eur. J.*, 2007, **13**, 8660–8666.
164 R. A. Miller, A. D. Presley and M. B. Francis, *J. Am. Chem. Soc.*, 2007, **129**, 3104–3109.
165 Y. Z. Ma, R. A. Miller, G. R. Fleming and M. B. Francis, *J. Phys. Chem. B*, 2008, **112**, 6887–6892.
166 L. M. Scolaro, M. A. Castriciano, A. Romeo, N. Micali, N. Angelini, C. Lo Passo and F. Felici, *J. Am. Chem. Soc.*, 2006, **128**, 7446–7447.